

Permafrost microbial communities follow shifts in vegetation, soils, and megafauna extinctions in Late Pleistocene NW North America

Tyler J. Murchie^{1,2,3} | George S. Long^{1,4} | Brian D. Lanoil⁵ | Duane Froese⁶ | Hendrik N. Poinar^{1,2,7,8,9}

¹McMaster Ancient DNA Centre,
 McMaster University, Hamilton, Ontario,
 Canada

²Department of Anthropology, McMaster
 University, Hamilton, Ontario, Canada

³Hakai Institute, Heriot Bay, British
 Columbia, Canada

⁴Department of Biology, McMaster
 University, Hamilton, Ontario, Canada

⁵Department of Biological Sciences,
 University of Alberta, Edmonton, Alberta,
 Canada

⁶Department of Earth and Atmospheric
 Sciences, University of Alberta,
 Edmonton, Alberta, Canada

⁷Department of Biochemistry, McMaster
 University, Hamilton, Ontario, Canada

⁸Michael G. DeGroote Institute for
 Infectious Disease Research, McMaster
 University, Hamilton, Ontario, Canada

⁹CIFAR, Humans and the Microbiome
 Program, MaRS Centre, Toronto, Ontario,
 Canada

Correspondence

Tyler J. Murchie, Hakai Institute, Heriot
 Bay, BC V0P 1H0, Canada.
 Email: tyler.murchie@hakai.org

Funding information

Belmont Forum; Biodiversa+; CANA
 Foundation; Natural Sciences and
 Engineering Research Council of Canada

Abstract

We analyzed the microbial constituent of sedimentary ancient DNA sequence data recovered from subarctic loessal permafrost sediments dating between 30,000 and 4000 years ago. These data were originally studied for paleo-ecological shifts in plants and animals associated with the Pleistocene–Holocene transition. Here, we explore whether there were changes in microbial communities paralleling the transition from distinctive cold-adapted Ice Age megafauna and vegetation communities—the mammoth steppe ecosystem—toward the expansion of woody shrubs, extirpation of grazing megaherbivores, and development of the boreal forest. We observe a clear shift in the relative proportions of prokaryotic taxa after ca. 13,300 years ago associated with the collapse of the mammoth steppe. These data are consistent among study sites and between replicates processed with different methodologies (shotgun sequencing and targeted capture), which highlights that the “off-target” fraction of metagenomic data used to study macro-ecosystems can also be used to investigate synchronous changes in microbial communities. Functional analyses were performed with SEED and KEGG databases where we observed a shift in methane metabolism pathways after ~13,100 years ago, which suggests that there was a shift in methanogenesis away from animal gut microflora at the end of the Pleistocene. There does not appear to be a significant shift in the overall diversity of microbial communities despite the observed taxonomic and functional changes.

KEY WORDS

extinction, Klondike, mammoth steppe, methanogens, permafrost microbial communities, Pleistocene–Holocene transition, sedimentary ancient DNA, woolly mammoths

1 | INTRODUCTION

The Pleistocene–Holocene transition (ca. 11,700 years ago) resulted in continental-scale biogeographic range shifts in ecological

communities of plants and animals (Bakker, Gill, et al., 2016; Bakker, Pagès, et al., 2016; Brault et al., 2013; Doughty et al., 2013, 2015, 2016; Guthrie, 1990, 1995, 2006; Malhi et al., 2016; Monteath et al., 2021, 2023; Murchie, Monteath, et al., 2021; Smith et al., 2015;

This is an open access article under the terms of the [Creative Commons Attribution](#) License, which permits use, distribution and reproduction in any medium, provided the original work is properly cited.

© 2023 The Authors. *Environmental DNA* published by John Wiley & Sons Ltd.

Wang, Pedersen, et al., 2021; Willerslev et al., 2014). From at least the Last Glacial Maximum (LGM, 26,500–19,000 years before present [BP]) (Clark, 2009) until the end of the Late Pleistocene, the northern hemisphere was populated by cold- and dry-adapted flora and fauna as part of what is generally referred to as the mammoth steppe biome (Froese et al., 2009; Graf, 2008; Guthrie, 2001; Hoffecker et al., 2014; Hopkins et al., 1982; Kuzmina et al., 2011; Zazula et al., 2003; Zimov et al., 2012). The mammoth steppe is characterized as being predominated by graminoids (grasses and sedges), forbs (herbaceous flowering plants like *Artemisia*), and megafauna (animals with a body mass ≥ 44 kg) such as woolly mammoths (*Mammuthus primigenius*), steppe bison (*Bison priscus*), and horses (*Equus caballus*), in parallel with a contingent of smaller fauna like arctic ground squirrels (*Urocitellus parryii*) and a lower abundance patchwork of woody shrubs (*Betula* and *Salix*). The mammoth steppe ecosystem has no direct modern analog, although Pavelková Říčánková et al. (2014) and Chytrý et al. (2019) argue that the Altai-Sayan Range along the border regions of Siberia, China, Kazakhstan, and Mongolia may approximate aspects of this now extinct biome. Likewise, the mega-faunal community diversity and estimated biotic productivity of the Late Pleistocene Holarctic (northern Eurasia, Beringia, and North America) have been compared with remaining areas of faunal gigantism such as East Africa (Bakker, Gill, et al., 2016; Guthrie, 1982; Malhi et al., 2016; Zimov et al., 2012). The turnover of flora, fungi, and animals during this transition between cold and warm stages of the late Quaternary has been studied widely across the northern hemisphere with macro-fossils (i.e., bones/teeth/soft tissues, plant remains, and arthropod exoskeletons), micro-fossils (i.e., environmental DNA, pollen, and fungal spores), and biogeochemical markers (i.e., isotopes and mineralogical/chemical profiles) (Mann et al., 2013; Meltzer, 2020; Monteath et al., 2021; Stuart, 2015). A relatively understudied aspect in this literature, however, is assessing to what degree prokaryotic communities (Bacteria and Archaea) also shifted in response to the glacial-to-interglacial transition and the associated shift in eukaryotic communities (Burkert et al., 2019; D'Costa et al., 2011; Liang et al., 2019; Mackelprang et al., 2011, 2017; Saidi-Mehrabad et al., 2020).

Saidi-Mehrabad et al. (2020) investigated this microbial community turnover with six permafrost sediments split between the Early Holocene (~8000–10,500 calibrated/calendar years before present [cal yr BP]) and Late Pleistocene (~14,300–16,000 cal yr BP) with amplicons of the 16S RNA gene, alongside chemical composition analyses of the associated sediments. They found significant taxonomic differences between Holocene- and Pleistocene-aged microbial communities along with changes in soil chemical profiles and other edaphic properties. Our goal was to expand on the study of Saidi-Mehrabad et al. (2020) by investigating structural and functional changes in microbial communities during this transition using metagenomic sedimentary ancient DNA (sedaDNA) data originally collected to study macro-ecological shifts associated with the collapse of the mammoth steppe ecosystem in Murchie, Monteath, et al. (2021).

To this end, we analyzed the microbial component of 99 sedaDNA libraries extracted from 21 permafrost cores from four sites

in central Yukon with previously documented shifts in macro-ecological communities using shotgun sequencing and capture enrichment (Figure 1, Table S1) (Murchie, Monteath, et al., 2021; Murchie, Kuch, et al., 2021; Murchie et al., 2022). Those sedaDNA data reconstructed a graminoid and forb dominated steppe-tundra ecosystem with a diversity of grazing megafauna from ca. 30,000 to 13,500 cal BP. This was followed by an ecological replacement with the expansion of woody shrubs and mesic tundra communities, along with the appearance of novel Eurasian cervid browsers (*Alces alces* and *Cervus canadensis*), followed by the eventual extirpation (local extinction) of grazing megafauna, increases in shrub thicket and forest-dwelling fauna, followed by the expansion of coniferous trees (*Picea* spp.) and development of the boreal forest (Figure 1). SedaDNA sequence data from Murchie, Monteath, et al. (2021); Murchie, Kuch, et al. (2021); Murchie et al. (2022) had been processed with two different extraction methods—the DNeasy PowerSoil extraction kit (QIAGEN) and Murchie, Kuch, et al.'s (2021) cold spin extractions—along with both shotgun sequencing and targeted capture. Capture enrichment was carried out first with the PalaeoChip Arctic v1.0 bait set, which was designed to enrich for ancient organellar genomes (mitochondria and chloroplast) from Holarctic flora and fauna (Murchie, Kuch, et al., 2021), in addition to baits designed to capture bovid mitogenomic DNA (such as steppe bison, American bison, yak, and Dall sheep) (Murchie et al., 2022). Wang, Pedersen, et al. (2021) observed the same ecological turnover as Murchie and colleagues—in terms of timings, taxonomic replacement, and the late survival signal of grazing megafauna including woolly mammoths (*Mammuthus primigenius*) and caballine horses (*Equus caballus*)—using shotgun sequenced sedaDNA from eastern Beringia (Alaska/Yukon) and from sites across the circumarctic.

Here, we use the taxonomically identified prokaryotic sedaDNA from Murchie, Monteath, et al. (2021), Murchie, Kuch, et al. (2021), and Murchie et al. (2022) libraries to assess whether there were shifts in microbial communities that were coeval with the macro-ecological transition in the Klondike goldfields of central Yukon, Canada. We use a combination of taxonomic cluster analyses, differential read abundances, diversity indices, damage analyses, co-occurrence, and correlation plots, along with functional analyses using KEGG and SEED databases to assess changes to the structure and function of microbial communities through the Pleistocene–Holocene transition in subarctic Yukon. Thereafter, we use these data to comment on the debate regarding sedaDNA evidence for the late survival of grazing herbivores (such as woolly mammoths and North American horses) into the early-to-middle Holocene (Arnold et al., 2011; Haile et al., 2009; Miller & Simpson, 2022; Murchie, Monteath, et al., 2021; Wang et al., 2022; Wang, Pedersen, et al., 2021).

2 | MATERIALS AND METHODS

Our dataset includes 99 sedaDNA libraries extracted with multiple biological replicates from 21 permafrost cores originating from

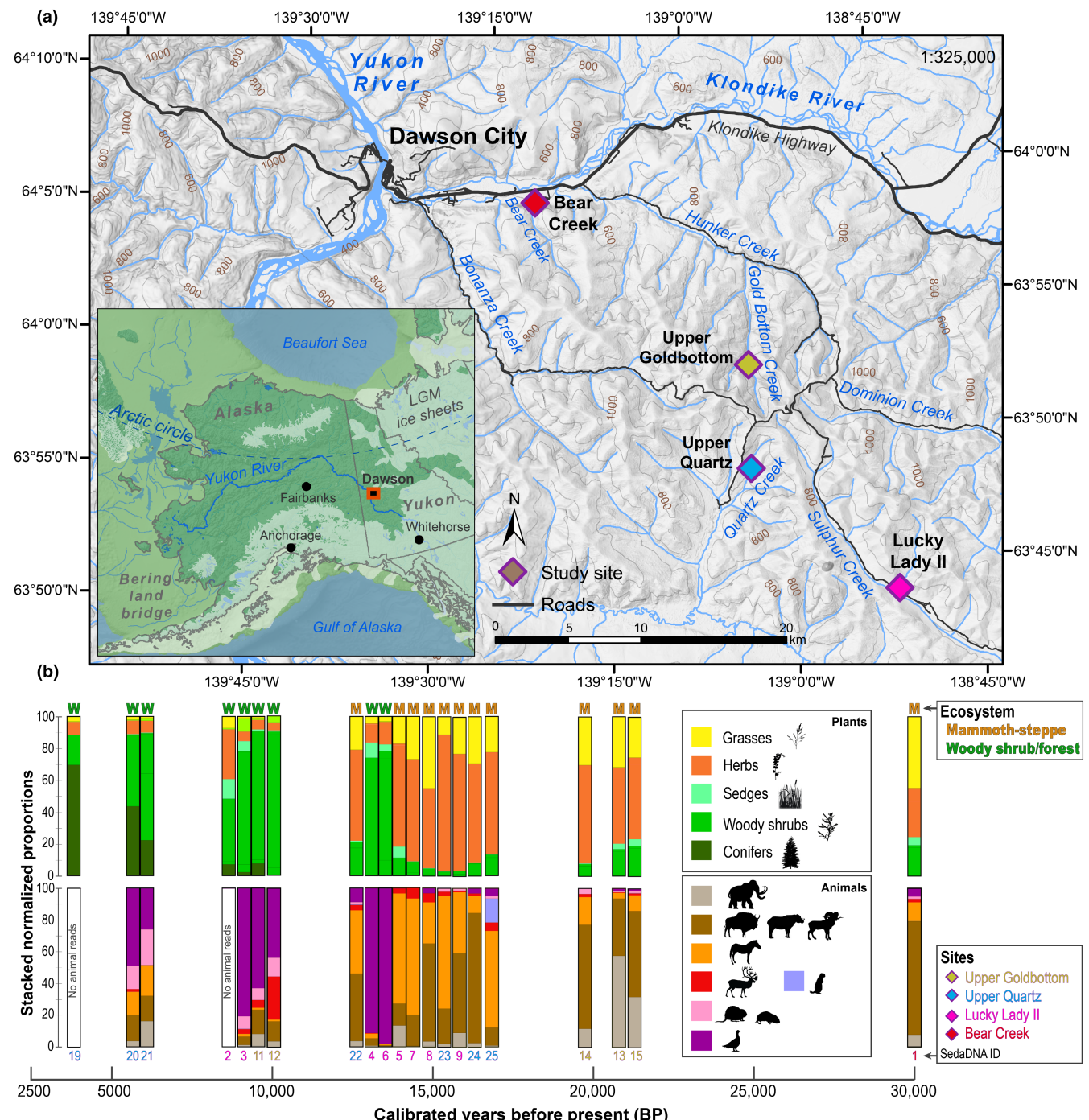


FIGURE 1 Study sites southwest of Dawson City, Yukon in the Klondike Goldfields. (a) Base map data from GeoYukon (Government of Yukon); contours in meters above sea level. Inset: Beringia during the last glacial maximum (LGM, 26.5–19 thousand years before present [ka BP]) (Clark, 2009). Ice sheet data from Dyke (2004). Sea level during LGM set to 126 m below sea level based on Clark and Mix (2002). Beringian paleo-drainage data from Bond (2019). (b) Macro-ecological sedimentary ancient DNA (sedaDNA) sequence data reprocessed from Murchie, Monteath, et al. (2021); Murchie et al. (2022) and summarized to major eukaryotic families. Wider x-axis spacing added between bars in ~15,000 BP cluster to remove visual bar overlap.

four sites in central Yukon, Canada (Figure 1, Table S1) (Murchie et al., 2022; Murchie, Kuch, et al., 2021; Murchie, Monteath, et al., 2021). This dataset also includes 26 negative controls processed alongside batches from these previous research efforts. For detailed descriptions of field sampling, ancient DNA (aDNA) wet lab processing, Bayesian age-depth modeling, palynology,

and other associated processing protocols and analyses, please see Murchie, Monteath, et al. (2021); Murchie, Kuch, et al. (2021); Murchie et al. (2022); D'Costa et al. (2011), Mahony (2015), and Sadoway (2014). Tables and figures referenced here with an S prefix (e.g., Table S1, Figure S2) can be found in the Supplementary Materials.

2.1 | Pre-sequencing summary

Twenty-one core samples of loessal permafrost silts were originally recovered in the field by D'Costa et al. (2011), Mahony (2015), and Sadoway (2014) between June and August of 2007, 2010, 2012, and 2013 with research permits issued to DF from the Yukon Heritage Branch, and through long-term community consultations with the placer gold mining community of the Klondike and the Tr'ondëk Hwëch'in Government. Sampling was conducted at placer gold mining exposures chosen for the quality of the exposure and expected age of the sediments. Horizontal permafrost cores were collected from the sites Bear Creek (BC), Upper Quartz (UQ), and Upper Goldbottom (UBG); vertical cores were taken from Lucky Lady II (LL2). The cores were kept in frozen storage at the McMaster Ancient DNA Centre (McMaster University) and the Permafrost Archives Laboratory (University of Alberta) until Murchie (2021) began reanalyzing these materials in ca. 2017. Prior to sample collection by all three original research teams, the sampling area was cleared of eroded materials back to frozen sediments to create a fresh coring surface for a ~10-cm-diameter coring tube up to ~30cm in length. Core samples were drilled with a small portable gas-powered drill (Echo), recovered frozen, stored individually in plastic bags, immediately placed in a -20°C chest freezer, and transported in the freezer to the University of Alberta or McMaster University for subsampling and analysis.

Ancient DNA laboratory work was conducted in clean rooms at the McMaster Ancient DNA Centre, which is subdivided into dedicated facilities for sample preparation, stock solution setup, and DNA extraction through library preparation. The post-indexing clean room (used for capture enrichment) is in a physically isolated workspace, and the subsequent high-copy PCR workspace is in a separate building. The center has a unidirectional workflow progressing from low-copy to high-copy facilities to reduce the chance of cross-contamination. Each dedicated workspace is physically separated with air pressure gradients between rooms to reduce airborne contamination. Prior to all phases of laboratory work, dead air hoods, and workspaces were cleaned using a 6% solution of sodium hypochlorite (commercial bleach), followed by a wash with Nanopure purified water (Barnstead) and 30 minutes of UV irradiation at >100mJ/cm².

Cores were subsampled in a dedicated sampling workspace with bleach, heat, and UV-sterilized equipment, tools, and counters. Subsamples were only taken from core interiors and care was taken to ensure that none of the sampling tools or interior surfaces were exposed to any materials that had come in physical contact with the core exteriors (that may contain mixed sedaDNA). Negative control blanks were used with every batch of subsamples/extractions at a ratio of at least 1 blank per 10 samples. Lysis and purification followed the extraction method described in Murchie, Kuch, et al. (2021)—utilizing a proteinase K digestion buffer and PowerBead lysing with a sedaDNA-modified high-volume silica-binding buffer and cold-spin inhibitor removal (Dabney, Knapp, et al., 2013; Karpinski et al., 2016; Murchie, Kuch, et al., 2021)—with sediment inputs ranging from 0.15 to 0.3 grams (wet weight). Double-stranded libraries were prepared as described by Meyer and Kircher (2010) and Kircher et al. (2012).

In-solution enrichments were carried out using a modified version of the myBaits v4.1 protocol (Daicel Arbor Biosciences) utilizing the PalaeoChip Arctic v1.0 bait set (Murchie, Kuch, et al., 2021), which targets whole mitochondrial genomes (~16,000 base pairs [bp]) of ~180 extinct and extant Holarctic fauna, along with the chloroplast genes *trnL*, *rbcL*, and *matK* (total ~2000 bp per species) from approximately 2100 species of Holarctic plants. Libraries were pooled to roughly equimolar concentrations and size selected with gel excision following electrophoresis for molecules ranging between 150 and 500bp. All libraries were sequenced on an Illumina HiSeq 1500 with either a 2×75 or 2×90 bp paired-end protocol at the Farncombe Metagenomics Facility (McMaster University, ON).

2.2 | Taxonomic and functional analyses

FASTQ files were demultiplexed with *bcl2fastq* (v1.8.4), converted to bam files with *fastq2bam* (https://github.com/grenaud/BCL2B_AM2FASTQ), and then trimmed and merged with *leeHom*¹⁸³ using ancient DNA-specific parameters (--ancientDNA). BAM files were converted to FASTA format, filtered for a minimum length of 24bp, filtered for any lingering similarity to sequencing adapters, and string deduplicated with the *NGSXRemoveDuplicates* module of NGSeXplore (<https://github.com/ktmeaton/NGSeXplore>). These filtered FASTAs were used as the input for two primary streams of taxonomic classification.

First with *MegaBLASTn* (Altschul et al., 1990) utilizing a July 2019 local copy of the GenBank NCBI (National Center for Biotechnology Information; Agarwala et al., 2016; Benson et al., 2013) nucleotide database set to return the top 50 alignments (unique accession hits) per read with e-values less than 1.0E-5 (flags: -num_alignments 50 -max_hsp 1 -evalue 0.00001). The outputs were passed to MEGAN (Ultimate Edition, v.6.24.4) (Huson et al., 2007, 2016) where the BLAST results were filtered through a lowest common ancestor (LCA) algorithm using the following parameters: *MinScore*=50.0; *MaxExpected*=1.0E-5; *MinPercentIdentity*=95.0; *TopPercent*=20.0; *MinSupport*=5; *LCA*=naïve; *MinPercentReadToCover*=80; and *mode*=*BlastN*. A secondary set of these *MegaBLASTn*/MEGAN classified reads were also generated where all species rank prokaryotic taxa identified in the blank control libraries were used as a background contamination filter to remove those hits from the analysis.

A second classification set was performed with DIAMOND v2.0.15.153 (Buchfink et al., 2021) in order to functionally classify the reads with SEED and KEGG databases (Kanehisa, 2019; Kanehisa et al., 2023; Kanehisa & Goto, 2000). DIAMOND was run with *BLASTx* using the NCBI RefSeq protein database (Release 214, September 16, 2022; flags: --unal 1 --query-cover 0.85 --subject-cover 0.85 -e 0.05 -k 100 -p 40 --sensitive). *BLASTx* classifications were passed to MEGAN (Ultimate Edition, v.6.24.4) using the February 2022 protein mapping database with the following LCA parameters: *MinScore*=50.0; *MaxExpected*=1.0E-5; *MinPercentIdentity*=95.0; *TopPercent*=10.0; *MinSupport*=5; *LCA*=naïve; *MinPercentReadToCover*=80; and *mode*=*BlastX*. A

secondary set of background negative control filters were also generated for these BLASTx/MEGAN classifications.

For both sets of taxonomic classification, libraries were compared in MEGAN and normalized to the total filtered reads of the smallest library. The normalizing factor in MEGAN is derived by dividing the read count of each taxonomic node by the total library reads, and then multiplying that by the total read count of the smallest library (Table S2). This normalization approach retains within-library proportions of taxonomic hits. Libraries with especially low-read counts after filtering and taxonomic assignment (less than 1 SD below the mean of total filtered reads) were excluded from the comparative analysis ($n=4/99$). Prokaryotic nodes within the comparisons were uncollapsed to species or genus ranks, libraries were color-coded based on macro-ecological community, and cluster analyses were performed in MEGAN using principal coordinate analyses (PCoA) and unrooted neighbor-joining trees with a χ^2 ecological index following the approach of Mitra et al. (2010).

2.3 | Damage analysis

A DIAMOND (Buchfink et al., 2021) search of the trimmed and merged reads was performed using a database of RefSeq proteins from 2023-02-10 (O'Leary et al., 2016). Successful hits required a 90% protein identity and an e-value $\leq 10^{-5}$ to be accepted. A lowest common ancestor (LCA) analysis of the results was then performed using an updated version of a previously published script (<https://github.com/longg2/LongBioinformatics>) (Hider et al., 2022). A 51% threshold was used to determine whether taxon could be assigned to a read. Cases where that was not possible were labeled as unknown reads. Candidate bacteria for the deamination and depurination analysis were then identified by selecting species that accounted for at least 1000 reads in a single sample. Four bacteria species—*Blastococcus endophyticus*, *Labilibacter sediminis*, *Paenarhrobacter nicotinovorans*, and *Solirubrobacter* sp. CPCC 204708—contained sufficient reads to warrant further analysis.

RefSeq genomes of the candidate bacteria were downloaded from NCBI using the NCBI datasets program. The samples were then mapped against the reference genomes using BWA *aln* (Li & Durbin, 2009) following previously published settings (Duggan et al., 2016). A minimum length of 24 bp and mapping quality of 30 was required for a read to be successfully matched. Successfully mapped reads then underwent coordinate-based deduplication using bam-rmdup (<https://bitbucket.org/ustenzel/biohazard-tools/src/master/>). This was then followed by estimating the level of deamination in the mapped reads using *mapDamage* 2.0 (Jónsson et al., 2013). Fragment length distributions (FLD) and mapping mismatches were also extracted from the deduplicated mapped reads.

The deamination and depurination analyses followed previously published methods (Kistler et al., 2017; Murchie, Monteath, et al., 2021). Unlike what has been done previously (Kistler et al., 2017; Murchie, Monteath, et al., 2021), the depurination of the sample was calculated through a linear regression of the \log_{10}

transformed FLDs ($\log_{10}(\text{Reads}) = \text{Read Length} * \text{Sample}$). Read lengths were filtered out from the linear regression if it accounted for less than 10 reads to prevent any outliers or insufficient data from affecting the results. Since the depurination rate is the slope of an exponential curve (Kistler et al., 2017), the specific values can be calculated by summing the coefficients of the read length as well as the interaction term for each sample. This method has the added benefit of being capable of determining the depurination level for multiple samples while also providing some statistical rigor to the slope by providing a *p*-value as well as an R^2_{adj} metric for the quality of the fits. A confidence interval for the slopes was also calculated through 1000 posterior simulations of the linear regression using the *arm R* package. Samples that had fewer than 1000 deduplicated reads mapping were also excluded from the analysis due to their low coverage.

The deamination and depurination rates were then compared to the estimated ages of the core samples. The macro-ecosystems of each sample (mammoth steppe, woody shrublands, and boreal forest) were used as proxies for both the age and climatic conditions. This is especially relevant as the mammoth steppe was more arid and cool than the Holocene-aged core samples from latter woody shrubland and boreal forest periods (Mann et al., 2013; Monteath et al., 2023; Zimov et al., 2012). A mixed linear model was used to control for the preservation effects conferred by the sampling location as well as the mapped bacteria in relation to both the deamination and depurination rates. The estimated ecosystem and the \log_{10} reads mapped were considered fixed effects, whereas the species and sampling sites were random effects.

3 | RESULTS

The sedaDNA classified prokaryotic communities from this dataset (Figure S1) consistently separate in cluster analyses by macro-ecological community (Figures 1 and 2). The first two principal components account for 48.7–80.2% of the variance in the data. This distinct clustering is observed both when assessing genus rank taxonomic hits in isolation (Figure 2) and when taking all prokaryotic assigned taxonomic ranks into consideration (Figure S2). Differences in the proportional representation of prokaryotes are found in high ranks such as Terrabacteria Group, and clades within including Actinobacteria/Actiomyctetes (phylum), Micrococcales (class), and Firmicutes (class) among others (Figure S3). More ecologically informative differences exist at the genus rank (Figure 3) where some taxa are more abundant reads during the Holocene shrub expansion, including the archaeal Methanobacteriaceae genera *Methanosarcina* and *Methanobacterium*, along with bacterial genera *Candidatus Nitrotoga*, and *Bacteriovorax*. Other prokaryotic genera appear more abundant during the Late Pleistocene mammoth steppe ecosystem, including *Cryobacterium*, *Alcaligenes*, *Escherichia*, *Arthrobacter*, *Pseudarthrobacter*, *Nocardioides*, *Rubrobacter*, *Desulfosporosinus*, and *Methanobrevibacter*. Amongst genus-ranked hits, 60.3% (182/302) of the prokaryotes have statistically significant differences (Table S3)

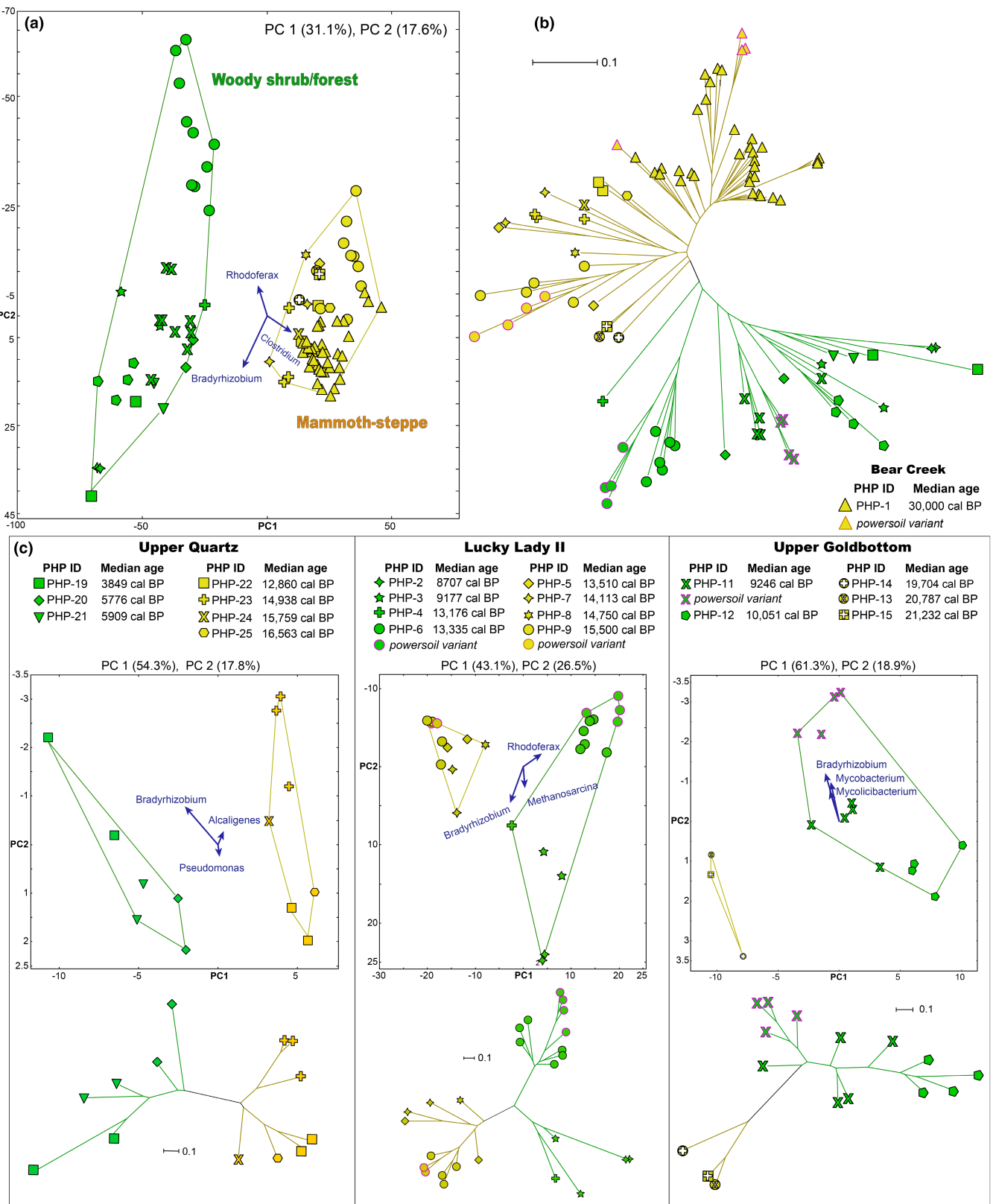


FIGURE 2 Cluster analyses of hits to Prokaryotic genera using a χ^2 ecological index. (a) PCoA of Prokaryotic genus rank hits from all libraries and study sites. Macro-ecological groups connected with convex hulls and color coded. (b) Unrooted neighbor-joining tree. (c) PCoAs and unrooted neighbor-joining trees for libraries separated by site. Bear Creek is excluded as all libraries from this site are replicates from a single sediment core sample.

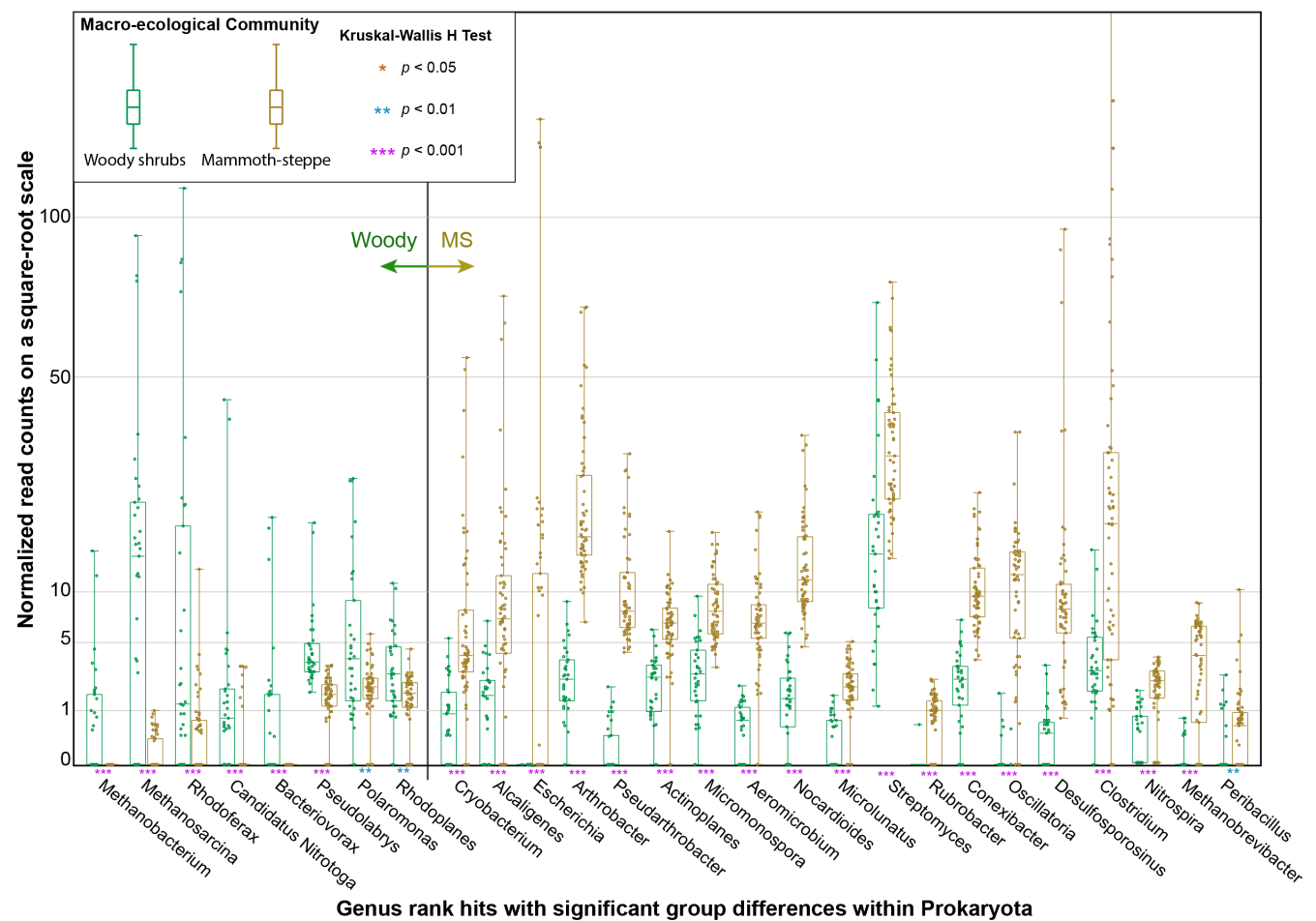


FIGURE 3 Boxplots of select prokaryotic genera with significant differences in taxonomic composition between the two macro-ecological groups. See Table S3 for the Kruskal–Wallis statistic table.

between the two main macro-ecological communities. These differences are consistent between biological replicates of the same cores completed with differing extraction and targeting approaches and are spatial-temporally consistent between sites in the region.

A co-occurrence analysis of genus rank nodes recapitulates the same major clusters of taxa driving structural differences in these two ecological communities (Figure S4). To ensure that background prokaryotic DNA (those deriving from plasticware, reagents, or other forms of potential contamination) are not driving any of these community differences, we performed these analyses again with all species observed in the negative controls removed and classified as “contaminants” (Table S4, Figures S6 and S7). Despite having 223 species-rank hits classified as background “contaminants” (many of which also reasonably originate from terrestrial sediments and hence their removal is highly conservative), the same bimodal clustering is observed with mammoth steppe libraries clustering separately from prokaryotes in the woody shrub libraries (Figure S8). The background DNA observed in our negative controls is consistently different from the predominant sedaDNA signal observed in our samples (Figure 4; Figure S9). This supports the authenticity of our sedaDNA reconstructions, implying that these signals originate from the sediments themselves and are not driven by contamination.

Rarefaction curves (Figure S10a) of prokaryotic taxa suggest that “mammoth steppe” sedaDNA libraries tend to be marginally more diverse than those from woody shrub periods. Average Shannon–Weaver and Simpson’s Reciprocal Diversity Indices support this difference in prokaryotic diversity (Figure S10c). However, when observing these data in a scatterplot (Figure S10b), it becomes clear that within-sample diversity estimates exceed any temporal or macro-ecological trends in shifting prokaryotic diversity. This suggests that microbial diversity overall did not shift significantly despite the clear transition of eukaryotic and prokaryotic communities.

Correlation plots (Figure 5; Figure S5) with hierarchical clustering of significantly differing prokaryotic and eukaryotic genera also recapitulate that communities of bacteria, archaea, fungi, plants, and animals cluster into two major groups—mammoth steppe and woody shrubland ecosystems—as we would expect based on previous research of the Late Pleistocene/Holocene transition in eastern Beringia (Guthrie, 2001; Monteath et al., 2021, 2023; Murchie, Monteath, et al., 2021; Wang, Pedersen, et al., 2021; Willerslev et al., 2014). Late Glacial megafauna (woolly mammoth, horse, bison, dall sheep, and caribou) correlate positively in these analyses with several bacteria (including *Clavibacter*, *Amycolatopsis*, *Micromonospora*, *Clostridium*, *Nitrospira*, *Anaeromyxobacter*, *Oscillatoria*, *Sporosarcina*,

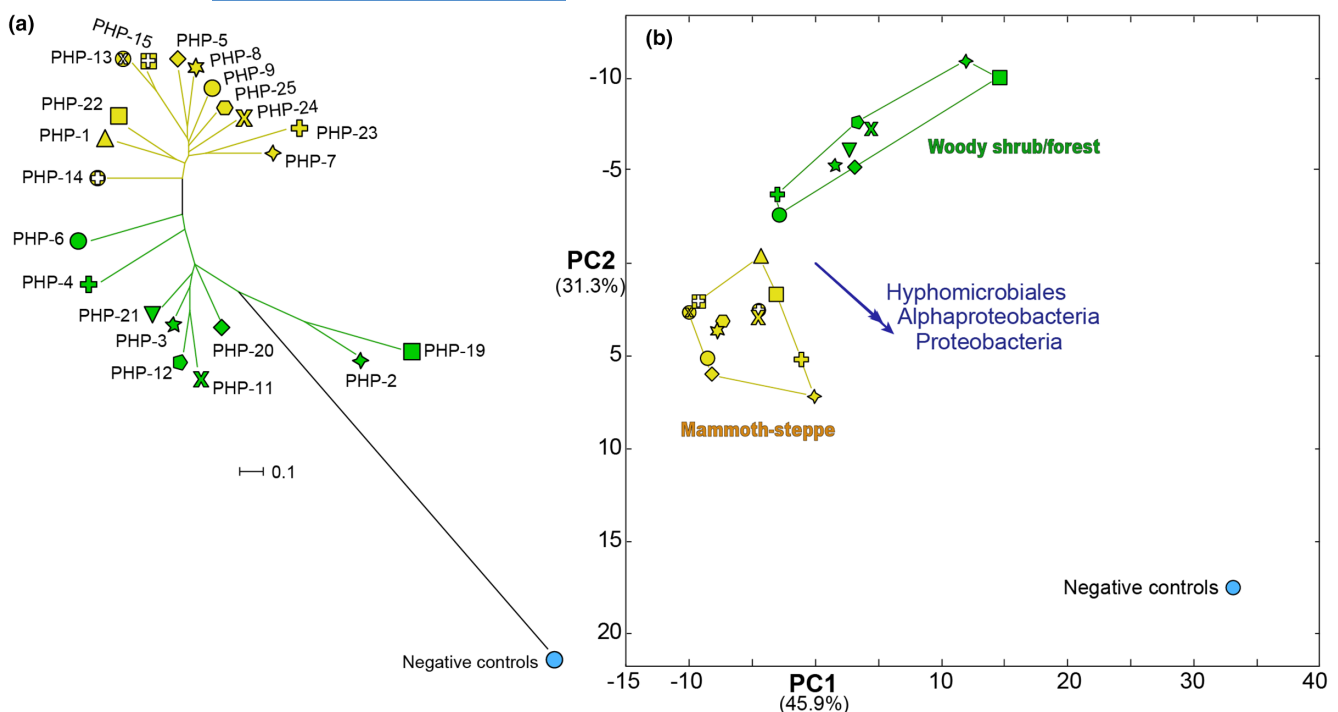


FIGURE 4 Merged negative controls compared with merged core replicates. Prokaryotic clades uncollapsed to species rank, all internal nodes selected for cluster analysis using a χ^2 ecological index. Normalized to smallest total read count. All plots were generated using the cluster analysis function in MEGAN. (a) Neighbor-joining tree of metagenomic spectra. (b) PCoA plot. See Figure S9 for associated UPGMA tree.

and *Pseudonocardia*), archaea (*Methanobrevibacter*), and plants (*Meconopsis* and *Papaver* [poppies], *Taraxacum* [dandelions], *Saxifraga* [rockfoils], and *Poaceae* [grasses]), along with other herbaceous and graminoid species and fungi (*Glarea*, *Endocarpion*, *Rhizophagus*, *Pleosporineae*). By contrast, Holocene animals [elk, moose, and hare] are not positively correlated with prokaryotes, although they are with the plants *Carex*, *Equisetum*, *Viburnum*, *Lupinus*, *Ribes*, *Vitis*, *Lupinus*, *Populus*, and *Salix*. The ground-dwelling bird *Lagopus* [ptarmigan] has positive correlations with the bacteria *Bacteriovorax*, *Agrobacterium*, *Flavobacterium*, *Acidovorax*, *Polaromonas*, and *Rhodoferax*.

This dataset suggests that there was a shift in methanogens from *Methanobrevibacter* spp. being predominant during ~30,000–15,000 calibrated/calendar years before present (cal BP), and their replacement by *Methanosarcina* spp. and *Methanobacterium* spp. after ~13,100 cal BP (Figure 8a,b; Figure S11). This is paralleled in our DIAMOND data with a functional shift in the KEGG methane metabolic pathway (Figure 6; Figures S13 and S14). Somewhat similar clustering is observed in nitrogen, sulfur, and carbon fixation pathways (Figure S12), although the clustering is not as distinct and largely disappears when we remove potential background species. Despite clear indications of major taxonomic shifts in microbial communities during this ecological transition, we observed few other functional differences with SEED and KEGG databases (Figures S15–S20).

Misincorporation plots, which are used to help differentiate between modern and ancient DNA (Dabney, Meyer, & Pääbo, 2013; Ginolhac et al., 2011; Jónsson et al., 2013), (Figure S21) have slight indications (relative to eukaryotic taxa) of deaminated nucleotides

on the termini of the sequenced reads. The reads are also all very short (24–31 bp). This may be due to insufficient coverage of the relatively large plastid genomes given that these are the off-target fraction of our sequenced reads, as well as abundant mis-mapping between related prokaryotes. There is also the possibility that long-term active repair mechanisms may minimize the deamination signal from prokaryotes (Johnson et al., 2007).

The mixed linear models indicate that the ecosystem had a significant effect on both depurination and deamination rates of identified adNA fragments (Figure 7). Specifically, they suggest that samples from the mammoth steppe had significantly less deamination than those from the boreal forest (95% confidence interval \log_{10} deamination rate: [0.084, 0.350]), whereas the shrublands acted as an intermediate environment (95% \log_{10} deamination rate: [-0.007, 0.209]). Similar results were obtained with the depurination rate, however, both the shrublands (95% \log_{10} depurination rate: [0.082, 0.232]) and the boreal forest (95% \log_{10} depurination rate: [0.078, 0.268]) were significantly different from the mammoth steppe. These results are in line with thermal-age models that suggest the environment of a sample has an important effect on DNA preservation (Hofreiter et al., 2015; Kistler et al., 2017; Smith et al., 2003), with the Holocene-aged cores coming from warmer, wetter periods where eDNA is more prone to hydrolytic forms of damage (Dabney, Meyer, & Pääbo, 2013). In both cases, the read counts did not have a significant effect on the damage rates (95% \log_{10} deamination: [-0.259, 0.082], 95% \log_{10} depurination: [-0.144, 0.021]). See the supplemental information for species-specific results (Figure S22).

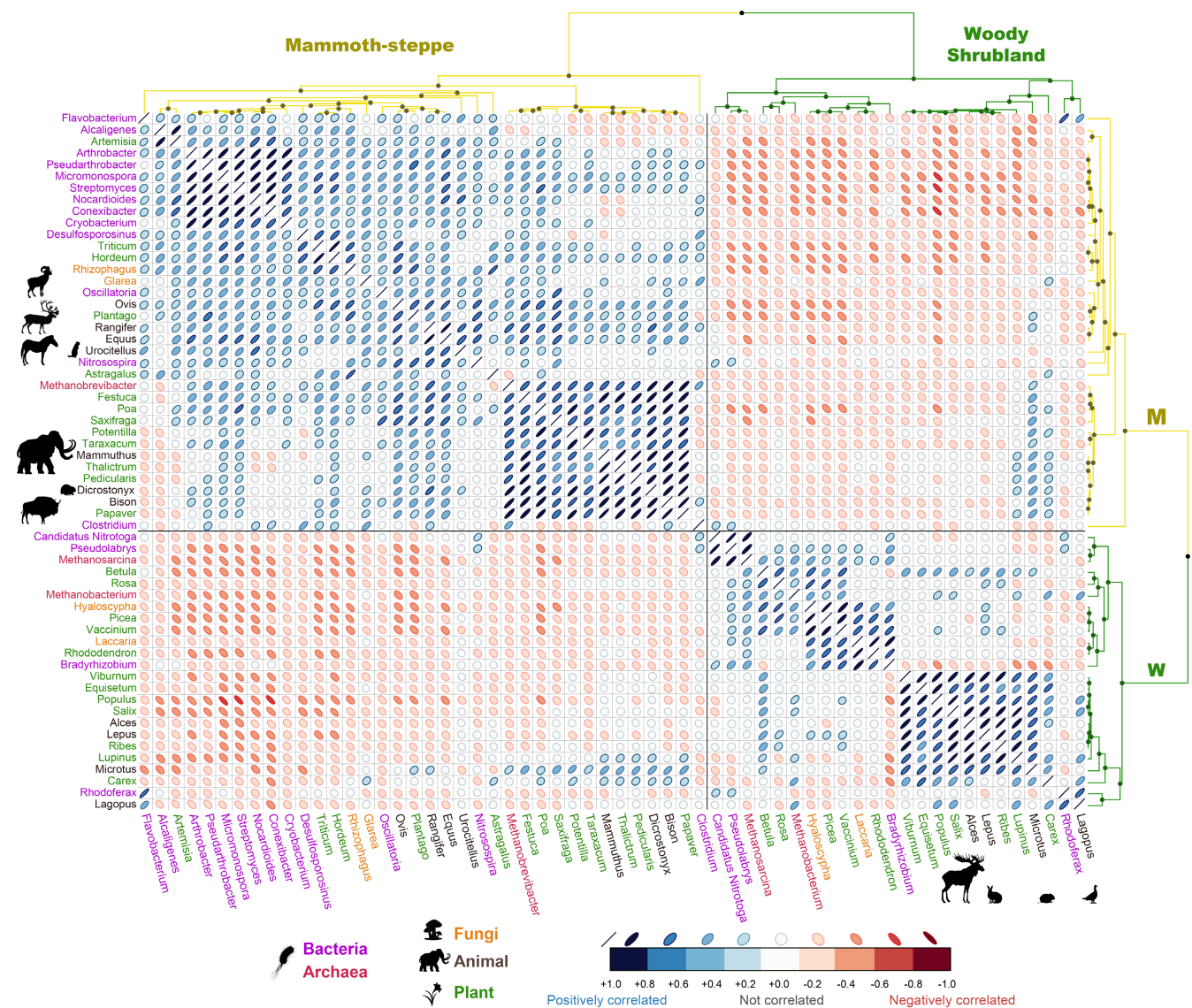


FIGURE 5 Correlation plot of select taxonomic nodes identified to co-occur significantly. Taxa ordered with hierarchical clustering. See Figure S5 for a larger correlation plot with additional taxa.

4 | DISCUSSION

An immediate challenge arises when interpreting shifting microbial taxa as to whether we can distinguish between the aDNA of preserved “relic” microbes (Carini et al., 2016; Lennon et al., 2018; Levy-Booth et al., 2007; Pedersen et al., 2015)—extracellular, fragmentary portions of long dead organisms that lived relatively contemporaneously with the eukaryotic aDNA under consideration here—versus long-lasting microbes that had been actively, but slowly, metabolizing and repairing in these permafrost samples for millennia (Johnson et al., 2007). Furthermore, the natural transformation of ancient microbial DNA has the potential to impact our taxonomic assignments if regions with taxonomically informative polymorphisms are transformed or laterally transferred to new microbial species that persisted in these sediments long after the initial deposition (Pedersen et al., 2015).

It generally appears that there is less deamination in our prokaryote-mapped reads than in those mapped to eukaryotes (Figure S21). This may suggest that some proportion of these microbes survived long after initial deposition, and as such, the community composition may have shifted. However, it should be noted that few bacterial species had sufficient coverage to properly analyze rates of deamination/depurination. In the case of four species with sufficient read depths, *Blastococcus endophyticus*, *Paenarthrobacter nicotinovorans*, and *Labilibacter sediminis* show evidence of increased damage (terminal base misincorporations and fragmentation) during woody shrubland and boreal forest periods (Figure 7; Figure S22). This is likely the result of increased moisture and temperature, causing more eDNA damage during tissue shedding prior to organo-mineral complex formation (Cai et al., 2006; Giguet-Covex et al., 2019; James Cleaves II et al., 2011; Murchie, Kuch, et al., 2021).

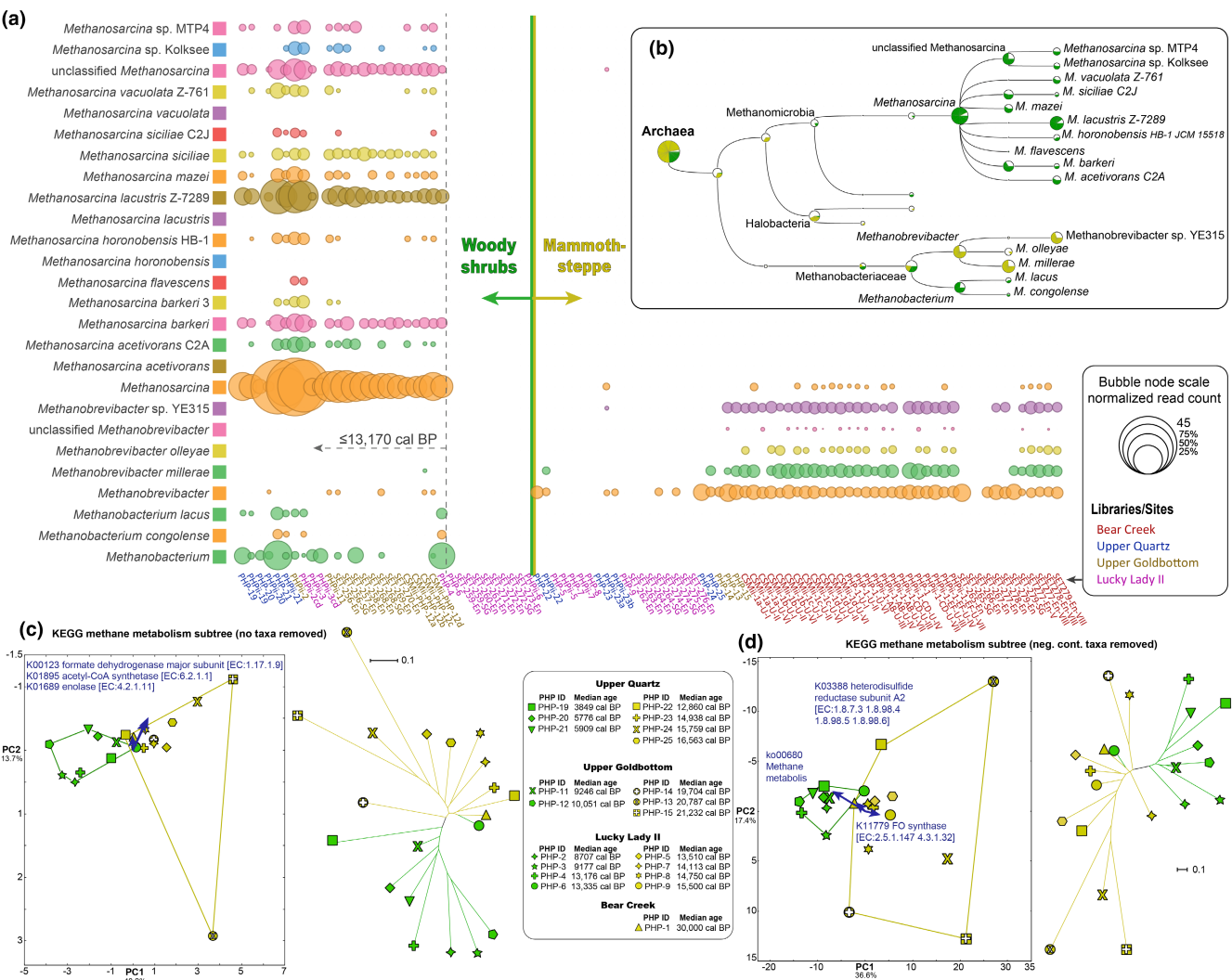


FIGURE 6 Methanogen shift associated with macro-ecological transition. (a) Bubble plot of normalized reads assigned to Archaeal methanogens (bubble size on a square-root scale). (b) MEGAN taxonomic tree of nodes from bubble plot. (c) KEGG PCoA and unrooted neighbor-joining tree of methane metabolism pathways plotted with a χ^2 ecological index with full dataset. (d) Same as (c) but with all species identified in the negative controls excluded.

Unfortunately, none of the taxa that significantly differ between the mammoth steppe and woody shrubland periods have sufficient mapped read depths to differentiate between long-term actively repairing microbes and relic, extracellular microbial DNA that was contemporaneous with the host deposit. Despite these limitations, there remains a significant distinction between microbial communities that is strongly correlated with the macro-ecological transition of eukaryotes from the mammoth steppe toward woody shrublands. The degree to which the taxonomic and functional specifics of how these communities may have been altered by long-persisting microbes is a question in need of further research.

4.1 | Structural and functional shifts in microbial communities

Our taxonomic cluster analyses parallel Saidi-Mehrabad et al. (2020) who found clear differences between Pleistocene- and

Holocene-aged prokaryotic communities. Genera more abundant from core samples dating to 30,000–14,000 cal BP include the cold-adapted, Gram-positive aerobes such as *Arthrobacter* (Han et al., 2021), *Pseudarthrobacter* (Shin et al., 2020), *Cryobacterium* (Liu et al., 2020), and *Friedmanniella* (Schumann et al., 1997), along with the sulfate-reducing *Desulfosporosinus* (Pester et al., 2012) and other soil-dwelling Bacteria and Archaea such as *Sporosarcina*, *Nocardioides*, *Conexibacter*, *Aeromicromyces*, and *Methanobrevibacter*. This also includes the somewhat unexpected recovery of the cyanobacterium *Oscillatoria* (Figures 4 and 5). While photoautotrophic microbes are typically associated with aquatic environments, viable cyanobacteria (including *Oscillatoria*) and green algae have been found in a range of extreme environmental conditions, including in ancient permafrost cores from the circumarctic (Vishnivetskaya, 2009; Vishnivetskaya et al., 2020). We observed positive correlations between bison sedaDNA and *Clostridium* (Figure 5; Figure S5), a gut microbe commonly found in bison, horse, and woolly mammoth fecal/coprolite samples

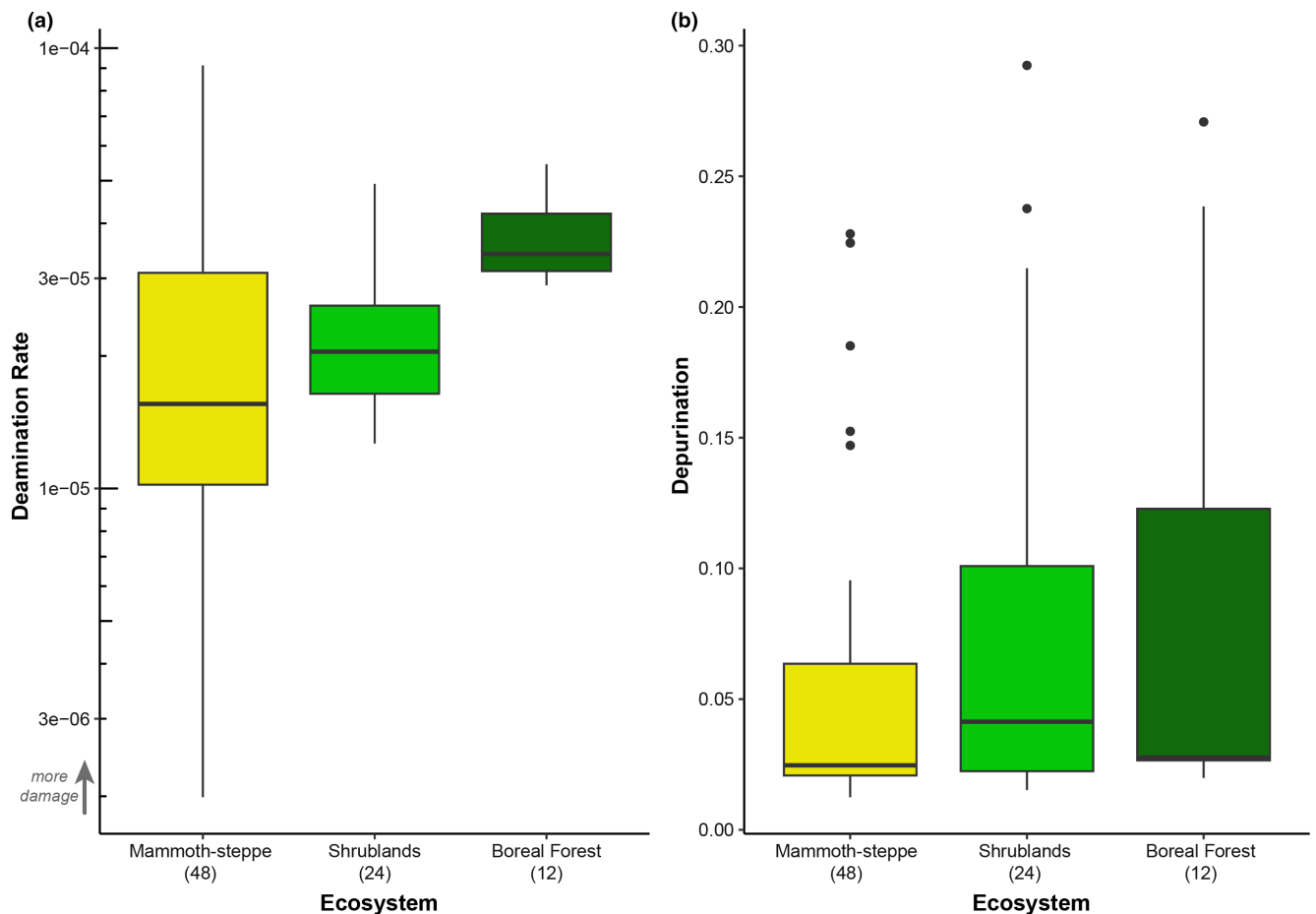


FIGURE 7 Summary of aDNA damage rates by macro-ecosystem. Pooled boxplots of (a) deamination rates and (b) depurination rates of the reads mapped to *Blastococcus endophyticus*, *Labilibacter sediminis*, *Paenarthrobacter nicotinovorans*, and *Solirubacter* spp. The number below each ecosystem indicates sample size. See also Figure S22.



FIGURE 8 Prokaryotic contribution to megafaunal late survival debate. Heatmap of select taxa with strongly partitioned distributions between mammoth steppe and woody shrub ecosystems (see also Figure S24).

(Kauter et al., 2019; Mardanov et al., 2012; Weese et al., 2014). However, *Clostridium* is found in most anaerobic environments, which is reflected in Figure 5 where *Clostridium* sits basal in the hierarchical clustering to the other mammoth-steppe-associated

taxa. Likewise, *Nitrospira*, an important component of the nitrogen cycle that can convert urea to ammonia (Koch et al., 2015; Spasov et al., 2020) has strong positive correlations with *Ovis*, *Equus*, and *Rangifer* in this dataset, but not with *Bison*, or

Mammuthus (Figure 5; Figure S5). Rather our *Bison*, *Mammuthus*, and *Discoctonyx sedaDNA* has strong positive correlations here with *Clavibacter*, *Amycolatopsis*, *Streptomyces*, *Micromonospora*, *Pseudonocardia*, *Methanobrevibacter*, and *Microlunatus*. These species have been found previously to be associated with either cold/ permafrost sediments (Deng et al., 2015; Gilichinsky et al., 2008; Wang, Wang, et al., 2021; Zaitseva et al., 2022) or Pleistocene megafauna (Jorns et al., 2020; van Bergeijk et al., 2022).

The degree to which any of these metagenomic correlations are ecologically causative, that is, due to a continuous abundance of large animal manure as a source of nitrogen and methane, among other compounds (Maeda et al., 2011), versus simply being correlated with the wider mammoth steppe ecosystem, is difficult to say at this time. The negative correlations observed among these and other 30,000–15,000 BP core-associated microbes indicate at minimum that these taxa are more associated with the mammoth steppe ecosystem, and less so with the subsequent expansion of woody shrublands (Figure 5; Figure S5).

The strong bimodal clustering by ecosystem that we observe here contrasts with the conclusions of Mackelprang et al. (2017) who argued that permafrost microbial community composition is not driven by vegetation dynamics based on their work on samples from the permafrost tunnels in Fox, Alaska. Their youngest sample (19,000–33,000 years ago) predates the ecological transition observed in this dataset, however. This likely explains their observed lack of macro-ecological correlations to microbial community shifts as their cores are too old to capture the shrubification of eastern Beringia and collapse of the mammoth steppe biome.

Murchie, Monteath, et al. (2021) and Monteath et al. (2023) observed a significant and rapid shift in multiple paleo-ecological proxies at the Lucky Lady site between 13,480 and 13,210 cal BP, corresponding here with samples PHP-5 (13,510 cal BP), PHP-6 (13,335 cal BP), and PHP-4 (13,176 cal BP). This period initially is associated with the development of a prominent paleosol, including the decline of steppe-tundra indicators like *Artemisia* spp. (sage, as indicated by both pollen and eDNA) and steppe weevil (*Connatichela artemisiae*), and their replacement by 13,210 cal BP with sedges (Cyperaceae), ground-nesting birds such as willow ptarmigan (*Lagopus lagopus*), and woody shrubs like *Salix*, *Alnus*, *Betula*, *Populus* and *Ericaceae* (Monteath et al., 2023; Murchie, Monteath, et al., 2021). It is during this transition in sample PHP-6 that we see an increase in the signals from the genera *Rhodoferax*, *Acidovorax*, and *Polaromonas*, with *Rhodoferax* being commonly associated with stagnant, waterlogged environments exposed to light (Hiraishi et al., 1991; Jin et al., 2020). These microbial shifts occur in association with substantial changes in pore-ice δ¹⁸O measurements at the site (Monteath et al., 2023), which together suggest a significant hydrological shift at the Lucky Lady site between 13,480 and 13,210 cal BP that is associated with wetter conditions, a shallowing of the active layer, and major taxonomic changes that have all been observed broadly across eastern Beringia associated with the expansion of shrubs (Mann et al., 2013, 2015; Monteath et al., 2021).

Despite the relatively rapid shift at the Lucky Lady site, the regional transition of the Klondike from mammoth steppe to woody shrubs was either somewhat gradual overall or was punctuated by the Younger Dryas cold interval (ca. 12,900–11,700 cal yr BP) (Rasmussen et al., 2006), which temporally sustained Late Glacial ecosystems. This is because sample PHP-22 from Upper Quartz post-dates the environmental transition at Lucky Lady II by ~300 years with a median modeled age of 12,860 cal BP (Table S1), and yet retains a macro- and micro-ecological sedaDNA signature characteristic of a mammoth steppe (Figures 1 and 2). Both sites are of equivalent elevation (Lucky Lady II: 615 meters above sea level [m asl]; Upper Quartz 620 m asl) (Mahony, 2015), and Upper Quartz is only 13 km northwest of Lucky Lady. Assuming the 2σ modeled ages are reasonably accurate for PHP-4/6/22 (see Murchie, Monteath, et al., 2021), these prokaryotic data support the interpretation by Murchie, Monteath, et al. (2021) that their single Younger Dryas core sample (PHP-22) suggests that the mammoth steppe ecosystem either persisted locally following Bølling-Allerød warming (ca. 14,690–12,900 cal BP) (Rasmussen et al., 2006), or reappeared during the Younger Dryas cooling.

Our samples that post-date this transition from the early Holocene (ca. 10,051–3849 cal yr BP) are associated with a decline in the relative proportions of many mammoth steppe typical microbes. Most notable is the prominent shift in methanogens from solely *Methanobrevibacter* during the Pleistocene toward *Methanobacterium* and *Methanosarcina* in the Holocene (Figure 6). *Methanobrevibacter* is a sister taxon to *Methanobacterium* (family Methanobacteriaceae) and members of these genera have similar metabolisms (an H₂-based reduction of CO₂) with *Methanobrevibacter* and *Methanobacterium* both being common gut microbes, and *Methanobacterium* also being common in freshwater sediments, swamps, and bogs (DasSarma et al., 2009). *Methanosarcina* by contrast is in a different Archaeal class, capable of growing on acetate, H₂, or methyl groups as electron donors (DasSarma et al., 2009; Ferry, 1997, 2020; Lessner et al., 2006; Weimer & Zeikus, 1978).

The methanogen shift we observe here is both taxonomic and functional, with the KEGG methane metabolic pathway showing a bimodal clustering among Holocene- and Pleistocene-aged samples. Notably, PHP-6 (13,335 cal yr BP) lacks any methanogen signal, whereas PHP-4 (13,176 cal BP) has an abrupt increase in *Methanobacterium* spp. and *Methanosarcina* spp. that continues through the remaining Holocene-aged core samples. *Methanobrevibacter* is commonly found not only in the gut microbiota of larger organisms, including the rumen of bovids and caprids (Lin et al., 1997), but also including many other animals and even insects like termites (Thomas et al., 2022). The lowest common ancestor (LCA) species classified in MEGAN for *Methanobrevibacter* are *M. olleyae*, *M. millerae*, and *Methanobrevibacter* sp. YE315. All three of these are derived from ovine and bovine rumen (Kelly et al., 2016; Ouwerkerk et al., 2011; Rea et al., 2007; Zhou, O'Hara, et al., 2021). Insect host-specific *Methanobrevibacter* such as *M. cuticularis* or *M. blatticola* were not identified (Brune, 2010). This suggests that

rumen-specific *Methanobrevibacter* may serve as a microbial indicator in our dataset of eastern Beringian bovids such as steppe bison (*Bison priscus*) and dall sheep (*Ovis dalli*). This association is supported by the abundance of Bovidae sedaDNA which is strongly correlated with *Methanobrevibacter* (Figure S5).

Methanosarcina, by contrast, is most positively correlated in our dataset not with animals but rather with the plant genera *Vaccinium* (shrubby heaths), *Betula* (birch), *Picea* (spruce), *Rhododendron* (shrub-to-tree heaths), *Sphagnum* (peat moss), *Hypnales* (feather moss), and *Hyaloscypha*, a fungus that lives symbiotically with species of *Betulaceae*, *Fagaceae*, *Pinaceae*, and *Salicaceae* (Fehrer et al., 2019)—all of which are common in our woody shrub period dataset, and are direct indicators of shrublands and a developing boreal forest (Figure 5; Figure S5). This correlation is likely not related causatively to these plant and fungal species, but rather to the changing hydrology of the region that also facilitated the growth of shrublands. LCA classifications within *Methanosarcina* include *M. lacustris* Z-7289, *M. mazei*, *M. siciliae*, *M. barkeri*, *M. acetivorans* C2A, and *Methanosarcina* sp. MTP4. This set includes both type I and type II species of *Methanosarcina*. While these two types have differing physiologies, they are found in a range of anaerobic semi-aquatic environments and moist soils such as swamps/bogs, sewage, muddy soils, ponds, and riverbeds, along with bovid rumen (Zhou, Holmes, et al., 2021). *Methanobacterium* is found in similar anaerobic environments such as lakes and peat bogs (Borrel et al., 2012; Cadillo-Quiroz et al., 2014).

The shift we observe in methanogens from *Methanobrevibacter* spp. during the Pleistocene to *Methanobacterium* spp. and *Methanosarcina* spp. during the Holocene may be a significant ecological indicator. *Methanobrevibacter* is a hydrogenotrophic methanogen—it can metabolize H₂—whereas *Methanosarcina* can use either H₂ or acetate as its energy source (depending on the species). The potential connection of *Methanobrevibacter* sedaDNA to gut microflora in this dataset (and the total absence of *Methanosarcina* in our >13,100 cal BP samples) might be indicative of there being a shift in soil methanogenesis at the end of the Pleistocene away from animal derived methane. The appearance of *Methanobacterium* spp. and *Methanosarcina* spp. after ~13,100 cal BP signifies a change in methanogenesis pathways with the onset of the Holocene associated with wetter conditions and woodland organisms. Only a small proportion of the total assigned reads are identified as methanogenic taxa (<0.2%, Figure S11). As such at this time, these indications are interesting datapoints highlighting an area in need of further research.

Despite having a combination of libraries extracted with two different methods, the DNeasy PowerSoil kit and sedaDNA-modified Dabney approach (Murchie, Kuch, et al., 2021), and three different sequencing targets—shotgun sequencing, PalaeoChip Arctic v1.0, and a Bovidae specific bait-set (Murchie, Monteath, et al. (2021); Murchie, Kuch, et al. (2021); Murchie et al. (2022))—all biological replicates cluster together (Figure 2; Figures S2 and S8). These varying approaches do result in subtle shifts in the microbial profiles as can be seen where PowerSoil extracts cluster together, as do shotgun

sequenced replicates. However, these replicates are more similar to those from the same core sample than other cores, irrespective of methodology. This helps further support the authenticity of our reconstructions, indicating that these sedaDNA signals originate from the sediments themselves and are not in any substantive way driven by contamination.

Our limited signal of metabolic functional differences may be the result of microbial niche replacement but is also likely impacted by insufficient sequencing depth and incomplete reference databases. Taxonomically among prokaryotes, the most deeply sequenced core sample (PHP-1), reached a species richness plateau in rarefaction curves at ~40 million filtered reads, with individual replicate libraries reaching a plateau at ~3.5 million reads in the shotgun library and between ~0.5 and 2 million reads in the PalaeoChip enriched libraries (Figure S23a,b). In contrast, none of the libraries reach a plateau in the KEGG rarefaction plots (Figure S23c,d). This indicates that to properly investigate shifting functional pathways, similar sedaDNA libraries would need to be sequenced as deep or deeper than PHP-1 (85 million reads with 37 replicates, Figure S23) with either many replicates or more complex libraries. Database incompleteness is also likely a factor; however, as in the MegaBLASTn taxonomic dataset, only 0.66% of 190 million combined reads could be assigned. Whereas with the BLASTp/DIAMOND dataset, 3% of the total combined reads were classified, a 4.6x increase. While the MegaBLASTn versus BLASTp classifier difference likely explains some of this variation in reads assigned, this more broadly highlights that as reference databases continue to expand, this dataset could be reanalyzed for improved taxonomic and functional analyses. A more comprehensive metagenomic reconstruction across all cores could be used to better understand how microbial communities recalibrated following the ecological transition from mammoth steppe ecosystems toward woody shrublands and forest. Such a reconstruction would allow for microbial comparisons with alleged mammoth steppe analogs such as Altai-Sayan range (Chytrý et al., 2019; Pavelková Říčánková et al., 2014) or African savannah (Bakker, Gill, et al., 2016; Malhi et al., 2016; Zimov et al., 2012), and may serve as a proxy indicator as to the holistic success of experimental reconstructions of a mammoth steppe analog at Pleistocene Park, Siberia (Fischer et al., 2022; Popov, 2020; Zimov, 2005).

4.2 | Assessing the contextual authenticity of Holocene-aged mammoth and horse sedaDNA

One of the unexpected findings from Murchie, Monteath, et al. (2021), Murchie, Kuch, et al. (2021), and Wang, Pedersen, et al. (2021) was the multi-site signal of megafaunal eDNA (woolly mammoths, woolly rhinoceros, and American horses) in sedimentary deposits younger than the last dated fossils of those species. We were interested here whether the prokaryotic component of this dataset could help inform the ongoing debate (Arnold et al., 2011; Haile et al., 2009; Miller & Simpson, 2022; Wang et al., 2022) on

megafaunal late survival as to whether there is evidence of mixed ecological signatures of microbial communities in our dataset that may indicate sedimentary reworking or bone seeding.

One cannot directly date individual DNA molecules, although with a sufficient abundance of sedaDNA from a particular species, one can use a Bayesian molecular clock to age estimate the composition and date of divergence of reassembled genomes (Gelabert et al., 2021; Kjær et al., 2022; Murchie et al., 2022; Pedersen et al., 2021; Vernot et al., 2021; Zavala et al., 2021; Zhang et al., 2020). In cases without exemplary preservation and recovery, such as with the trace signals of late-surviving megafauna from the Holocene-aged samples reported in Murchie, Monteath, et al. (2021), dating is entirely reliant on stratigraphic analysis and the radiometric dating of contextually associated organics. Within this dataset, Murchie, Monteath, et al. (2021); Murchie, Kuch, et al. (2021) found sedaDNA evidence for the late survival of caballine horse and woolly mammoth extending to ~10,000–9000 cal BP from multiple sites, and potentially even as late as 6000–5700 cal BP from their youngest samples. Wang, Pedersen, et al. (2021) found the same overall sedaDNA signal with a much larger, circumarctic dataset suggesting that mammoths survived until 7300 (mainland Siberia) and 8600 cal yr BP (North American), with horses potentially surviving in eastern Beringia until 7900 cal BP. Wang, Pedersen, et al. (2021) expanded on and reanalyzed samples from Haile et al. (2009), whose original Alaskan sedaDNA evidence found strong evidence for the survival of horses and mammoths until ca. 10,000 years ago. Based on dated macro-fossils (bones), horses and mammoths were thought to have disappeared from the mainland in Yukon and Alaska around 13,000 years ago. Research on Arctic islands such as Wrangel (Vartanyan et al., 2008) and St. Paul (Graham et al., 2016) have found strong evidence, including dated fossils, for mammoth survival until 5500 and 4000 years ago, respectively. As such, there is great interest in determining whether this late survival was relegated to Arctic islands or whether mainland refugia persisted elsewhere.

Three primary mechanisms have been proposed that may impact the contextual authenticity of sedaDNA. The first is leaching (Figure S24), which involves high-output eDNA sources (such as urination and carcass decomposition) percolating downward into older strata (Haile et al., 2007). This factor is unlikely to be of significance for the late survival question here, insofar as this mechanism results in younger DNA being mixed with older DNA, which would impact estimates on the arrival of a species, not their disappearance. And, because permafrost is thought to function as an aquitard or aquiclude (Woo, 2012), it is thought to render those perennially frozen layers largely impervious to the transmission of groundwater, hence limiting sedaDNA leaching. This is supported by $\delta^{18}\text{O}$ signatures in the area showing a lack of water migration (Monteath et al., 2023; Porter et al., 2019). This also supports the contextual authenticity of our mammoth-steppe-aged microbial community signals. Since the microbes would be migrating with the water, a lack of water migration means a lack of microbial movement between perennially frozen deposits.

More challenging to rule out are the processes of sediment reworking through erosion and redeposition (Figure S24) (Arnold

et al., 2011), and the proposed potential for surface bone persistence being an ongoing source of animal eDNA into ecosystems (Miller & Simpson, 2022). In the case of Murchie, Monteath, et al. (2021), reworking was argued to be unlikely to explain the late survival signal observed between sites because (1) the signal was identified in as many as 12 core samples from three separate sites spread over 40 km, which show a regionally consistent and abrupt shift in ecosystems during the Pleistocene–Holocene transition with no obvious evidence of stratigraphic mixing (at Lucky Lady 2 in particular) (Monteath et al., 2023). (2) The data had both age and climatologically associated DNA damage patterns. (3) Evidence of late survival has been found in multiple studies from the circumarctic (Vartanyan et al., 2008; Haile et al., 2009; Graham et al., 2016; Zazula et al., 2017; Murchie, Kuch, et al., 2021; Murchie, Monteath, et al., 2021; Wang, Pedersen, et al., 2021; Wang et al., 2022; Monteath et al., 2023). (4) The bone fossil record of Beringia is both inherently fragmentary and largely undated. And, (5) with an incomplete record, we would not expect to easily find fossil evidence of refugial populations due to the Signor–Lipps effect (Signor & Lipps, 1982). There are now multiple lines of evidence for the prolonged survival of grazing megafauna on the Beringian mainland until ~10,000–8000 BP.

If, however, remobilized sediments are the reason for megafaunal DNA persisting into Holocene deposits, we would expect to see eDNA from grasses, herbaceous plants, and small mammals such as ground squirrels, and mammoth steppe microbial DNA being reworked alongside eDNA from woolly mammoths and horses at similar local rates. Essentially, we would expect to see the late persistence of an entire ecosystem. Other than the allegedly late-surviving megafauna under question though, there is no evidence of any formerly omnipresent plant or animal species that entirely disappeared during the Pleistocene/Holocene transition in Yukon/Alaska that could be used to clearly indicate the genetic mixing of ecosystems from different time periods. Most organisms persisted through the Pleistocene–Holocene transition but with shifting proportions in Holocene communities.

This shift in abundance rather than presence/absence is also true for prokaryotes; however, we did observe at least five genera that are consistently present during the mammoth steppe period but are absent in samples where late-surviving horse and mammoth sedaDNA is identified (Figure 8). These are the bacterial genera *Pseudarthrobacter*, *Oscillatoria*, and *Desulfosporosinus*, the archaea *Methanobrevibacter*, and the plant *Taraxacum* (dandelions). While none of these exist at read abundances during the mammoth steppe that would classify them as robustly diagnostic indicators of reworking, they do function as supporting evidence that reworking appears to have contributed minimally to these ecological reconstructions, as otherwise these and other species that bimodally cluster in our libraries would be expected to be locally reworked at the same rate.

More broadly, however, if there was sedimentary reworking, we would expect our prokaryote cluster analyses to have significantly more overlap as we would expect a blurring of microbial signals between these two time periods. This is not what we observe—our microbial communities consistently separate into two distinct

clusters. These strongly partitioned signals argue against reworking being a significant variable in these data, and as such argue against late persisting megafaunal sedaDNA being the result of remobilized sediments.

Finally, Miller and Simpson (2022) critiqued Wang, Pedersen, et al.'s (2021) late survival data, arguing that the persistence of unburied bones on the surface of Arctic landscapes (as well as previously eroded carcasses) could be a source of continually disseminated eDNA into local environments that may result in faunal sedaDNA being reworked independent of other associated organisms such as plants and microbes. Their temperature-based model only predicted Pleistocene-aged bone surface persistence in North America until ca. 10,000, but if including later eroded bones that then persist on the surface for some unknown duration, this mechanism could theoretically conflate eDNA of differing time periods. Wang et al. (2022) argue against surface bone persistence (or "bone seeding") as being a major driver in their reconstructions on the basis of (1) expected declining haplotype diversity through time; (2) a lack of horizontal/vertical "smearing" of megafaunal DNA that would be expected with millennial scale bone persistence being a major source of eDNA; (3) the distinct unevenness of late survival signals suggesting small refugial populations; and (4) the complexity of factors involved in bone persistence beyond simply temperature (including carnivore/scavengers, constant exposure to UV and liquid water, seasonal freezing/thawing, and a range of other biogeochemical processes) that would be expected to rapidly degrade exposed surface bone aDNA even if the bones were to physically persist.

We cannot entirely rule out surface or eroded bones serving as a source of decontextualized ancient eDNA in this dataset. It seems unlikely, however, that aDNA from a single organism could ever be reworked independently of the associated microbial community. Eroded bones would be associated with eroded, relict microbial DNA from those earlier time periods. Likewise, bone seeding from never-buried bone would still have an associated microbiome that would be redeposited alongside those decontextualized animal aDNA fragments. The strong bimodal clustering of our microbial data supports the interpretation that reworking and bone seeding have contributed minimally (if at all) to our dataset. Deeper sequencing (>50 million reads per sample) would be necessary to explore the microbial signals here to the degree that the potential for reworking can be fully explored. Ongoing sedaDNA research from stratigraphically well-understood sites, especially lakes and entirely loessal deposits where temporal mixing (be it from reworked sediments or eroded/exposed bones) is highly improbable, will be key moving forward to confirm or refute the growing corpus of late-surviving megafaunal sedaDNA research. We argue on the basis of the results presented here that more holistic ecological analyses (looking at both eukaryotes and prokaryotes) with sedaDNA will be an important area of research moving forward for more fully understanding ecological turnovers, such as the Pleistocene–Holocene transition, along with smaller-scale regional complexities in biogeographic range shifts.

This dataset focused on prokaryotes mirrors the community turnover observed in macro-ecosystems across the Pleistocene/

Holocene transition. Microbial community composition shifted during the collapse of the mammoth steppe ecosystem as the environment underwent woody shrubification and paludification (development of peatlands) (Mann et al., 2013), along with the later development of boreal forest. These data were derived from two sedimentary DNA extraction protocols and three sequencing approaches, and yet biological replicates consistently cluster together. This underscores that microbial sedaDNA can be used to more holistically study paleo-ecosystems, even with a dataset originally intended for plant and animal sedaDNA. We observe a functional change in methane metabolic pathways that are correlated with shifting communities of plants, animals, and fungi. The correlation between *Methanobrevibacter* spp. and Pleistocene megafauna, along with the taxonomic transition toward *Methanobacterium* spp. and *Methanoscincina* spp. after 13,100 years ago, may be a significant ecological indicator of changing methanogenic pathways due to the loss of diverse and abundant megafauna, shifting vegetation, and wetter conditions. The consistent separation of microbial communities in this dataset between mammoth steppe and woody shrubland periods helps serve as supporting evidence for the contextual authenticity of late-surviving megafauna DNA in these samples, highlighting another aspect of sedaDNA that can be used moving forward as researchers attempt to resolve the ongoing debate regarding megafaunal late survival.

Broadly, these data highlight how the collapse of the mammoth steppe ecosystem affected all organisms in the Klondike region—from some of the largest land mammals that have ever existed, down to single-celled organisms. Such a complete ecological transition may prove conceptually useful for modeling and monitoring ongoing and future transitions in microbial communities to be expected with the current warming Arctic.

AUTHOR CONTRIBUTIONS

Conceptualization: Tyler J. Murchie, Duane Froese, and Hendrik N. Poinar. **Methodology:** Tyler J. Murchie and George S. Long. **Investigation:** Tyler J. Murchie, George S. Long, Brian D. Lanoil, Duane Froese, and Hendrik N. Poinar. **Visualization:** Tyler J. Murchie and George S. Long. **Supervision:** Duane Froese and Hendrik N. Poinar. **Writing—original draft:** Tyler J. Murchie. **Writing—review & editing:** Tyler J. Murchie, George S. Long, Brian D. Lanoil, Duane Froese, and Hendrik N. Poinar.

ACKNOWLEDGMENTS

Tyler J. Murchie and Hendrik N. Poinar wish to thank the CANA Foundation for their generous support of a PDF to Tyler J. Murchie along with associated laboratory operating costs. Thank you to the placer gold mining community of the Klondike and the Tr'ondëk Hwéch'in for their continued support of our research and access to study sites in the central Yukon. Thanks to Brian Golding for providing access to his computational resources, which were invaluable to the processing of these datasets. Thanks to all members and affiliates of the McMaster Ancient DNA Centre for their ongoing support, as well as the admin and faculty of the Anthropology and Biochemistry

departments at McMaster University. Thank you to the reviewers and editors at Environmental DNA for your time, consideration, and feedback. Finally, Tyler J. Murchie wishes to dedicate this work to the memory of Stewart Murchie who passed away during the writing of this manuscript.

FUNDING INFORMATION

This work was funded by the CANA Foundation, Belmont Forum, and BiodivERsA grants (to Duane Froese and Hendrik N. Poinar) for the Future ArcTic Ecosystems (FATE) research consortium, as well as NSERC Discovery grants to Duane Froese and Hendrik N. Poinar.

CONFLICT OF INTEREST STATEMENT

Authors declare that they have no competing interests.

DATA AVAILABILITY STATEMENT

All sequence data are deposited on the NCBI SRA under BioProject PRJNA1004851. Previously published data used in this report can be found on the NCBI SRA under BioProjects PRJNA752360 and PRJNA722670. PalaeoChip references and bait sequences used for the capture enrichment are available at <https://doi.org/10.5281/zenodo.5643845>.

ORCID

Tyler J. Murchie  <https://orcid.org/0000-0003-1104-4597>

REFERENCES

- Agarwala, R., Barrett, T., Beck, J., Benson, D. A., Bollin, C., Bolton, E., Bourexis, D., Brister, J. R., Bryant, S. H., Canese, K., Charowhas, C., Clark, K., Dicuccio, M., Dondoshansky, I., Federhen, S., Feolo, M., Funk, K., Geer, L. Y., Gorelenkov, V., ... Zbicz, K. (2016). Database resources of the National Center for Biotechnology information. *Nucleic Acids Research*, 44, D7–D19. <https://doi.org/10.1093/nar/gkv1290>
- Altschul, S. F., Gish, W., Miller, W., Myers, E. W., & Lipman, D. J. (1990). Basic local alignment search tool. *Journal of Molecular Biology*, 215, 403–410. [https://doi.org/10.1016/S0022-2836\(05\)80360-2](https://doi.org/10.1016/S0022-2836(05)80360-2)
- Arnold, L. J., Roberts, R. G., Macphee, R. D. E., Haile, J. S., Brock, F., Möller, P., Froese, D. G., Tikhonov, A. N., Chivas, A. R., Gilbert, M. T. P., & Willerslev, E. (2011). Paper II – Dirt, dates and DNA: OSL and radiocarbon chronologies of perennially frozen sediments in Siberia, and their implications for sedimentary ancient DNA studies. *Boreas*, 40, 417–445. <https://doi.org/10.1111/j.1502-3885.2010.00181.x>
- Bakker, E. S., Gill, J. L., Johnson, C. N., Vera, F. W., Sandom, C. J., Asner, G. P., & Svenning, J. C. (2016). Combining paleo-data and modern enclosure experiments to assess the impact of megafauna extinctions on woody vegetation. *Proceedings of the National Academy of Sciences of the United States of America*, 113, 847–855. <https://doi.org/10.1073/pnas.1502545112>
- Bakker, E. S., Pagès, J. F., Arthur, R., & Alcoverro, T. (2016). Assessing the role of large herbivores in the structuring and functioning of freshwater and marine angiosperm ecosystems. *Ecography*, 39, 162–179. <https://doi.org/10.1111/ecog.01651>
- Benson, D. A., Cavanaugh, M., Clark, K., Karsch-Mizrachi, I., Lipman, D. J., Ostell, J., & Sayers, E. W. (2013). GenBank. *Nucleic Acids Research*, 41, D36–D42. <https://doi.org/10.1093/nar/gks1195>
- Bond, J. D. (2019). Paleodrainage map of Beringia, Yukon geological survey. Open File 2019-2. <http://data.geology.gov.yk.ca/>
- Borrel, G., Joblin, K., Guedon, A., Colombe, J., Tardy, V., Lehours, A. C., & Fonty, G. (2012). *Methanobacterium lacus* sp. nov., isolated from the profundal sediment of a freshwater meromictic lake. *International Journal of Systematic and Evolutionary Microbiology*, 62, 1625–1629. <https://doi.org/10.1099/ijss.0.034538-0>
- Brault, M. O., Mysak, L. A., Matthews, H. D., & Simmons, C. T. (2013). Assessing the impact of late Pleistocene megafaunal extinctions on global vegetation and climate. *Climate of the Past*, 9, 1761–1771. <https://doi.org/10.5194/cp-9-1761-2013>
- Brune, A. (2010). Methanogens in the digestive tract of termites. In J. H. P. Hackstein (Ed.), *(Endo)symbiotic methanogenic archaea* (pp. 81–100). Springer.
- Buchfink, B., Reuter, K., & Drost, H. G. (2021). Sensitive protein alignments at tree-of-life scale using DIAMOND. *Nature Methods*, 18, 366–368. <https://doi.org/10.1038/s41592-021-01101-x>
- Burkert, A., Douglas, T. A., Waldrop, M. P., & Mackelprang, R. (2019). Changes in the active, dead, and dormant microbial community structure across a pleistocene permafrost chronosequence. *Applied and Environmental Microbiology*, 85, e02646-18. <https://doi.org/10.1128/AEM.02646-18>
- Cadillo-Quiroz, H., Brauer, S. L., Goodson, N., Yavitt, J. B., & Zinder, S. H. (2014). *Methanobacterium paludis* sp. nov. and a novel strain of *Methanobacterium lacus* isolated from northern peatlands. *International Journal of Systematic and Evolutionary Microbiology*, 64, 1473–1480. <https://doi.org/10.1099/ijss.0.059964-0>
- Cai, P., Huang, Q., Zhang, X., & Chen, H. (2006). Adsorption of DNA on clay minerals and various colloidal particles from an Alfisol. *Soil Biology and Biochemistry*, 38, 471–476. <https://doi.org/10.1016/j.soilbio.2005.05.019>
- Carini, P., Marsden, P. J., Leff, J. W., Morgan, E. E., Strickland, M. S., & Fierer, N. (2016). Relic DNA is abundant in soil and obscures estimates of soil microbial diversity. *Nature Microbiology*, 2, 1–6. <https://doi.org/10.1038/nmicrobiol.2016.242>
- Chytrý, M., Horská, M., Danihelka, J., Ermakov, N., German, D. A., Hájek, M., Hájková, P., Kočí, M., Kubešová, S., Lustyk, P., Nekola, J. C., Pavelková Řičánková, V., Preislerová, Z., Resl, P., & Valachovič, M. (2019). A modern analogue of the Pleistocene steppe-tundra ecosystem in southern Siberia. *Boreas*, 48, 36–56. <https://doi.org/10.1111/BOR.12338>
- Clark, P. U., & Mix, A. C. (2002). Ice sheets and sea level of the last glacial maximum. *Quaternary Science Reviews*, 21, 1–7.
- Clark, P. U. (2009). The last glacial maximum. *Science*, 325, 710–714. <https://doi.org/10.1126/science.1172873>
- Dabney, J., Knapp, M., Glocke, I., Gansauge, M.-T., Weihmann, A., Nickel, B., Valdiosera, C., Garcia, N., Arsuaga, J.-L., & Meyer, M. (2013). Complete mitochondrial genome sequence of a middle Pleistocene cave bear reconstructed from ultrashort DNA fragments. *Proceedings of the National Academy of Sciences of the United States of America*, 110, 15758–15763. <https://doi.org/10.1073/pnas.1314445110>
- Dabney, J., Meyer, M., & Pääbo, S. (2013). Ancient DNA damage. *Cold Spring Harbor Perspectives in Biology*, 5, 1–7. <https://doi.org/10.1101/cshperspect.a012567>
- DasSarma, S., Coker, J. A., & DasSarma, P. (2009). Archaea (overview). In M. Schaechter (Ed.), *Encyclopedia of microbiology* (pp. 1–23). Academic Press.
- D'Costa, V. M., King, C. E., Kalan, L., Morar, M., Sung, W. W. L., Schwarz, C., Froese, D., Zazula, G., Calmels, F., Debruyne, R., Golding, G. B., Poinar, H. N., & Wright, G. D. (2011). Antibiotic resistance is ancient. *Nature*, 477, 457–461. <https://doi.org/10.1038/nature10388>
- Deng, J., Gu, Y., Zhang, J., Xue, K., Qin, Y., Yuan, M., Yin, H., He, Z., Wu, L., Schuur, E. A. G., Tiedje, J. M., & Zhou, J. (2015). Shifts of tundra bacterial and archaeal communities along a permafrost thaw gradient in Alaska. *Molecular Ecology*, 24, 222–234. <https://doi.org/10.1111/MEC.13015>

- Doughty, C. E., Faurby, S., & Svenning, J. C. (2016). The impact of the megafauna extinctions on savanna woody cover in South America. *Ecography*, 39, 213–222. <https://doi.org/10.1111/ecog.01593>
- Doughty, C. E., Roman, J., Faurby, S., Wolf, A., Haque, A., Bakker, E. S., Malhi, Y., Dunning, J. B., & Svenning, J.-C. (2015). Global nutrient transport in a world of giants. *Proceedings of the National Academy of Sciences of the United States of America*, 113, 1–6. <https://doi.org/10.1073/pnas.1502549112>
- Doughty, C. E., Wolf, A., & Malhi, Y. (2013). The legacy of the Pleistocene megafauna extinctions on nutrient availability in Amazonia. *Nature Geoscience*, 6, 761–764. <https://doi.org/10.1038/ngeo1895>
- Duggan, A. T., Perdomo, M. F., Piombino-Mascali, D., Marciak, S., Poinar, D., Emery, M. V., Buchmann, J. P., Duchêne, S., Jankauskas, R., Humphreys, M., Golding, G. B., Southon, J., Devault, A., Rouillard, J. M., Sahl, J. W., Dutour, O., Hedman, K., Sajantila, A., Smith, G. L., ... Poinar, H. N. (2016). 17th century variola virus reveals the recent history of smallpox. *Current Biology*, 26, 3407–3412. <https://doi.org/10.1016/j.cub.2016.10.061>
- Dyke, A. S. (2004). An outline of the deglaciation of North America with emphasis on central and northern Canada. *Developments in Quaternary Sciences*, 2, 373–424.
- Fehrer, J., Réblová, M., Bambasová, V., & Vohník, M. (2019). The root-symbiotic Rhizoscyphus ericae aggregate and Hyaloscypha (Leotiomycetes) are congeneric: Phylogenetic and experimental evidence. *Studies in Mycology*, 92, 195–225. <https://doi.org/10.1016/J.SIMYCO.2018.10.004>
- Ferry, J. G. (1997). Enzymology of the fermentation of acetate to methane by *Methanosarcina thermophila*. *BioFactors*, 6, 25–35. <https://doi.org/10.1002/BIOF.5520060104>
- Ferry, J. G. (2020). Methanosarcina acetivorans: A model for mechanistic understanding of Acetilastic and reverse methanogenesis. *Frontiers in Microbiology*, 11, 1806. <https://doi.org/10.3389/FMICB.2020.01806>
- Fischer, W., Thomas, C. K., Zimov, N., & Göckede, M. (2022). Grazing enhances carbon cycling but reduces methane emission during peak growing season in the Siberian Pleistocene Park tundra site. *Biogeosciences*, 19, 1611–1633. <https://doi.org/10.5194/bg-19-1611-2022>
- Froese, D. G., Zazula, G. D., Westgate, J. A., Preece, S. J., Sanborn, P. T., Reyes, A. V., & Pearce, N. J. G. (2009). The Klondike goldfields and Pleistocene environments of Beringia. *GSA Today*, 19, 4–10. <https://doi.org/10.1130/GSATG54A.1>
- Gelabert, P., Sawyer, S., Bergström, A., Margaryan, A., Collin, T. C., Meshveliani, T., Belfer Cohen, A., Lordkipanidze, D., Jakeli, N., Matskevich, Z., Bar-Oz, G., Fernandes, D. M., Cheronet, O., Özdogan, K. T., Oberreiter, V., Feeney, R. N. M., Stahlschmidt, M. C., Skoglund, P., Pinhasi, R., ... Pinhasi, R. (2021). Genome-scale sequencing and analysis of human, wolf, and bison DNA from 25,000-year-old sediment. *Current Biology*, 31, 3564–3574. <https://doi.org/10.1016/j.cub.2021.06.023>
- Giguët-Covex, C., Ficetola, G. F., Walsh, K., Poulenard, J., Bajard, M., Fouinat, L., Sabatier, P., Gielly, L., Messenger, E., Develle, A. L., David, F., Taberlet, P., Brisset, E., Guiter, F., Sinet, R., & Arnaud, F. (2019). New insights on lake sediment DNA from the catchment: Importance of taphonomic and analytical issues on the record quality. *Scientific Reports*, 9, 1–21. <https://doi.org/10.1038/s41598-019-50339-1>
- Gilichinsky, D., Vishnivetskaya, T., Petrova, M., Spirina, E., Mamykin, V., & Rikvina, E. (2008). Bacteria in permafrost. In R. Margesin, F. Schinner, J. Marx, & C. Gerday (Eds.), *Psychrophiles: From biodiversity to biotechnology* (pp. 83–102). Springer.
- Ginolhac, A., Rasmussen, M., Gilbert, M. T. P., Willerslev, E., & Orlando, L. (2011). mapDamage: Testing for damage patterns in ancient DNA sequences. *Bioinformatics*, 27, 2153–2155. <https://doi.org/10.1093/bioinformatics/btr347>
- Graf, K. E. (2008). *Uncharted territory: Late Pleistocene hunter-gatherer dispersals in the Siberian mammoth-steppe*. University of Nevada.
- Graham, R. W., Belmecheri, S., Choy, K., Culleton, B. J., Davies, L. J., Froese, D., Heintzman, P. D., Hritz, C., Kapp, J. D., Newsom, L. A., Rawcliffe, R., Saulnier-Talbot, É., Shapiro, B., Wang, Y., Williams, J. W., & Wooller, M. J. (2016). Timing and causes of mid-Holocene mammoth extinction on St. Paul Island, Alaska. *Proceedings of the National Academy of Sciences of the United States of America*, 113, 9310–9314. <https://doi.org/10.1073/pnas.1604903113>
- Guthrie, D. R. (1982). Mammals of the mammoth steppe as paleoenvironmental indicators. In D. M. Hopkins, J. V. J. Matthews, C. E. Schweger, & S. B. Young (Eds.), *Paleoecology of beringia* (pp. 307–326). Academic Press.
- Guthrie, R. D. (1990). *Frozen fauna of the mammoth steppe: The story of blue babe*. University of Chicago Press.
- Guthrie, R. D. (1995). Mammalian evolution in response to the Pleistocene–Holocene transition and the break-up of the mammoth steppe: two case studies. *Acta Zoologica Cracoviensia*, 38, 139–154.
- Guthrie, R. D. (2001). Origin and causes of the mammoth steppe: A story of cloud cover, woolly mammal tooth pits, buckles, and inside-out Beringia. *Quaternary Science Reviews*, 20, 549–574. [https://doi.org/10.1016/S0277-3791\(00\)00099-8](https://doi.org/10.1016/S0277-3791(00)00099-8)
- Guthrie, R. D. (2006). New carbon dates link climatic change with human colonization and Pleistocene extinctions. *Nature*, 441, 207–209. <https://doi.org/10.1038/nature04604>
- Haile, J., Froese, D. G., MacPhee, R. D. E., Roberts, R. G., Arnold, L. J., Reyes, A. V., Rasmussen, M., Nielsen, R., Brook, B. W., Robinson, S., Demuro, M., Gilbert, M. T. P., Munch, K., Austin, J. J., Cooper, A., Barnes, I., Möller, P., & Willerslev, E. (2009). Ancient DNA reveals late survival of mammoth and horse in interior Alaska. *Proceedings of the National Academy of Sciences of the United States of America*, 106, 22352–22357. <https://doi.org/10.1073/pnas.0912510106>
- Haile, J., Holdaway, R., Oliver, K., Bunce, M., Gilbert, M. T. P., Nielsen, R., Munch, K., Ho, S. Y. W., Shapiro, B., & Willerslev, E. (2007). Ancient DNA chronology within sediment deposits: Are paleobiological reconstructions possible and is DNA leaching a factor? *Molecular Biology and Evolution*, 24, 982–989. <https://doi.org/10.1093/molbev/msm016>
- Han, S. R., Kim, B., Jang, J. H., Park, H., & Oh, T. J. (2021). Complete genome sequence of *Arthrobacter* sp. PAMC25564 and its comparative genome analysis for elucidating the role of CAZymes in cold adaptation. *BMC Genomics*, 22, 1–14. <https://doi.org/10.1186/S12864-021-07734-8>
- Hider, J., Duggan, A. T., Klunk, J., Eaton, K., Long, G. S., Karpinski, E., Giuffra, V., Ventura, L., Fornaciari, A., Fornaciari, G., Golding, G. B., Prowse, T. L., & Poinar, H. N. (2022). Examining pathogen DNA recovery across the remains of a 14th century Italian friar (Blessed Sante) infected with *Brucella melitensis*. *International Journal of Paleopathology*, 39, 20–34. <https://doi.org/10.1016/J.IJPP.2022.08.002>
- Hiraishi, A., Hoshino, Y., & Satoh, T. (1991). *Rhodoferax fermentans* gen. Nov., sp. nov., a phototrophic purple nonsulfur bacterium previously referred to as the “*Rhodococcus gelatinosus*-like” group. *Archives of Microbiology*, 155, 330–336. <https://doi.org/10.1007/BF00243451>
- Hoffecker, J. F., Elias, S. A., & Rourke, D. H. O. (2014). Out of beringia? *Science*, 343, 979–980.
- Hofreiter, M., Pajtmans, J. L. A., Goodchild, H., Speller, C. F., Barlow, A., Fortes, G. G., Thomas, J. A., Ludwig, A., & Collins, M. J. (2015). The future of ancient DNA: Technical advances and conceptual shifts. *BioEssays*, 37, 284–293. <https://doi.org/10.1002/BIES.201400160>
- Hopkins, D. M., Matthews, J. V., & Schweger, C. E. (Eds.). (1982). *Paleoecology of beringia*. Academic Press.
- Huson, D. H., Auch, A. F., Qi, J., & Schuster, S. C. (2007). MEGAN analysis of metagenomic data. *Genome Research*, 17, 377–386. <https://doi.org/10.1101/gr.5969107>

- Huson, D. H., Beier, S., Flade, I., Górska, A., El-Hadidi, M., Mitra, S., Ruscheweyh, H. J., & Tappu, R. (2016). MEGAN community edition - interactive exploration and analysis of large-scale microbiome sequencing data. *PLoS Computational Biology*, 12, e1004957. <https://doi.org/10.1371/journal.pcbi.1004957>
- James Cleaves, H., II, Crapster-Pregont, E., Jonsson, C. M., Jonsson, C. L., Sverjensky, D. A., & Hazen, R. A. (2011). The adsorption of short single-stranded DNA oligomers to mineral surfaces. *Chemosphere*, 83, 1560–1567. <https://doi.org/10.1016/j.chemosphere.2011.01.023>
- Jin, C. Z., Zhuo, Y., Wu, X., Ko, S. R., Li, T., Jin, F. J., Ahn, C. Y., Oh, H. M., Lee, H. G., & Jin, L. (2020). Genomic and metabolic insights into denitrification, sulfur oxidation, and multidrug efflux pump mechanisms in the bacterium *Rhodoferax sediminis* sp. nov. *Microorganisms*, 8, 262. <https://doi.org/10.3390/MICROORGANISMS8020262>
- Johnson, S. S., Hebsgaard, M. B., Christensen, T. R., Mastepanov, M., Nielsen, R., Munch, K., Brand, T., Gilbert, M. T. P., Zuber, M. T., Bunce, M., Rønn, R., Gilichinsky, D., Froese, D., & Willerslev, E. (2007). Ancient bacteria show evidence of DNA repair. *Proceedings of the National Academy of Sciences of the United States of America*, 104, 14401–14405. <https://doi.org/10.1073/pnas.0710637105>
- Jónsson, H., Ginolhac, A., Schubert, M., Johnson, P. L. F., & Orlando, L. (2013). MapDamage2.0: Fast approximate Bayesian estimates of ancient DNA damage parameters. *Bioinformatics*, 29, 1682–1684. <https://doi.org/10.1093/bioinformatics/btt193>
- Jorns, T., Craine, J., Towne, E. G., & Knox, M. (2020). Climate structures bison dietary quality and composition at the continental scale. *Environmental DNA*, 2, 77–90. <https://doi.org/10.1002/EDN3.47>
- Kanehisa, M. (2019). Toward understanding the origin and evolution of cellular organisms. *Protein Science*, 28, 1947–1951. <https://doi.org/10.1002/PRO.3715>
- Kanehisa, M., Furumichi, M., Sato, Y., Kawashima, M., & Ishiguro-Watanabe, M. (2023). KEGG for taxonomy-based analysis of pathways and genomes. *Nucleic Acids Research*, 51, D587–D592. <https://doi.org/10.1093/NAR/GKAC963>
- Kanehisa, M., & Goto, S. (2000). KEGG: Kyoto encyclopedia of genes and genomes. *Nucleic Acids Research*, 28, 27–30. <https://doi.org/10.1093/NAR/28.1.27>
- Karpinski, E., Mead, J. I., & Poinar, H. N. (2016). Molecular identification of paleofeces from Bechan cave, southeastern Utah, USA. *Quaternary International*, 443, 140–146. <https://doi.org/10.1016/j.quaint.2017.03.068>
- Kauter, A., Epping, L., Semmler, T., Antao, E.-M., Kannapin, D., Stoeckle, S. D., Gehlen, H., Lübke-Becker, A., Günther, S., Wieler, L. H., & Walther, B. (2019). The gut microbiome of horses: Current research on equine enteral microbiota and future perspectives. *Animal Microbiome*, 1, 1–15. <https://doi.org/10.1186/S42523-019-0013-3>
- Kelly, W. J., Pacheco, D. M., Li, D., Attwood, G. T., Altermann, E., & Leahy, S. C. (2016). The complete genome sequence of the rumen methanogen *Methanobrevibacter millerae* SM9. *Standards in Genomic Sciences*, 11, 1–9. <https://doi.org/10.1186/S40793-016-0171-9>
- FIGURES/4**
- Kircher, M., Sawyer, S., & Meyer, M. (2012). Double indexing overcomes inaccuracies in multiplex sequencing on the Illumina platform. *Nucleic Acids Research*, 40, 1–8. <https://doi.org/10.1093/nar/gkr771>
- Kistler, L., Ware, R., Smith, O., Collins, M., & Allaby, R. G. (2017). A new model for ancient DNA decay based on paleogenomic meta-analysis. *Nucleic Acids Research*, 45, 6310–6320. <https://doi.org/10.1093/nar/gkx361>
- Kjær, K. H., Winther Pedersen, M., De Sanctis, B., De Cahsan, B., Korneliussen, T. S., Michelsen, C. S., Sand, K. K., Jelavić, S., Ruter, A. H., Schmidt, A. M. A., Kjeldsen, K. K., Tesakov, A. S., Snowball, I., Gosse, J. C., Alsos, I. G., Wang, Y., Dockter, C., Rasmussen, M., Jørgensen, M. E., ... Willerslev, E. (2022). A 2-million-year-old ecosystem in Greenland uncovered by environmental DNA. *Nature*, 612, 283–291. <https://doi.org/10.1038/s41586-022-05453-y>
- Koch, H., Lücker, S., Albertsen, M., Kitzinger, K., Herbold, C., Speck, E., Nielsen, P. H., Wagner, M., & Daims, H. (2015). Expanded metabolic versatility of ubiquitous nitrite-oxidizing bacteria from the genus *Nitrospira*. *Proceedings of the National Academy of Sciences of the United States of America*, 112, 11371–11376. <https://doi.org/10.1073/PNAS.1506533112>
- Kuzmina, S. A., Sher, A. V., Edwards, M. E., Haile, J., Yan, E. V., Kotov, A. V., & Willerslev, E. (2011). The late Pleistocene environment of the eastern west Beringia based on the principal section at the Main River, Chukotka. *Quaternary Science Reviews*, 30, 2091–2106. <https://doi.org/10.1016/j.quascirev.2010.03.019>
- Lennon, J. T., Muscarella, M. E., Placella, S. A., & Lehmkühl, B. K. (2018). How, when, and where relic DNA affects microbial diversity. *MBio*, 9, e00637-18. <https://doi.org/10.1128/MBIO.00637-18>
- Lessner, D. J., Li, L., Li, Q., Rejtár, T., Andreev, V. P., Reichlen, M., Hill, K., Moran, J. J., Karger, B. L., & Ferry, J. G. (2006). An unconventional pathway for reduction of CO₂ to methane in CO-grown *Methanosarcina acetivorans* revealed by proteomics. *Proceedings of the National Academy of Sciences of the United States of America*, 103, 17921–17926. <https://doi.org/10.1073/PNAS.0608833103>
- Levy-Booth, D. J., Campbell, R. G., Gulden, R. H., Hart, M. M., Powell, J. R., Klironomos, J. N., Pauls, K. P., Swanton, C. J., Trevors, J. T., & Dunfield, K. E. (2007). Cycling of extracellular DNA in the soil environment. *Soil Biology and Biochemistry*, 39, 2977–2991. <https://doi.org/10.1016/J.SOILBIO.2007.06.020>
- Li, H., & Durbin, R. (2009). Fast and accurate short read alignment with burrows-wheeler transform. *Bioinformatics (Oxford, England)*, 25, 1754–1760. <https://doi.org/10.1093/bioinformatics/btp324>
- Liang, R., Lau, M., Vishnivetskay, T., Lloyd, K. G., Wang, W., Wiggins, J., Miller, J., Pfiffner, S., Rivkina, E. M., & Onstott, T. C. (2019). Predominance of anaerobic, spore-forming bacteria in metabolically active microbial communities from ancient Siberian permafrost. *Applied and Environmental Microbiology*, 85, e00560-19. <https://doi.org/10.1128/AEM.00560-19>
- Lin, C., Raskin, L., & Stahl, D. A. (1997). Microbial community structure in gastrointestinal tracts of domestic animals: Comparative analyses using rRNA-targeted oligonucleotide probes. *FEMS Microbiology Ecology*, 22, 281–294. <https://doi.org/10.1111/J.1574-6941.1997.TB00380.X>
- Liu, Y., Shen, L., Zeng, Y., Xing, T., Xu, B., & Wang, N. (2020). Genomic insights of *Cryobacterium* isolated from ice core reveal genome dynamics for adaptation in glacier. *Frontiers in Microbiology*, 11, 1530. <https://doi.org/10.3389/FMICB.2020.01530>
- Mackelprang, R., Burkert, A., Haw, M., Mahendrarajah, T., Conaway, C. H., Douglas, T. A., & Waldrop, M. P. (2017). Microbial survival strategies in ancient permafrost: Insights from metagenomics. *The ISME Journal*, 11, 2305–2318. <https://doi.org/10.1038/ISMEJ.2017.93>
- Mackelprang, R., Waldrop, M. P., Deangelis, K. M., David, M. M., Chavarria, K. L., Blazewicz, S. J., Rubin, E. M., & Jansson, J. K. (2011). Metagenomic analysis of a permafrost microbial community reveals a rapid response to thaw. *Nature*, 480, 368–371. <https://doi.org/10.1038/nature10576>
- Maeda, K., Hanajima, D., Toyoda, S., Yoshida, N., Morioka, R., & Osada, T. (2011). Microbiology of nitrogen cycle in animal manure compost. *Microbial Biotechnology*, 4, 700–709. <https://doi.org/10.1111/J.1751-7915.2010.00236.X>
- Mahony, M. E. (2015). 50,000 years of paleoenvironmental change recorded in meteoric waters and coeval paleoecological and cryostratigraphic indicators from the Klondike goldfields, Yukon, Canada. University of Alberta.

- Malhi, Y., Doughty, C. E., Galetti, M., Smith, F. A., Svenning, J.-C., & Terborgh, J. W. (2016). Megafauna and ecosystem function from the Pleistocene to the Anthropocene. *Proceedings of the National Academy of Sciences of the United States of America*, 113, 838–846. <https://doi.org/10.1073/pnas.1502540113>
- Mann, D. H., Groves, P., Kunz, M. L., Reanier, R. E., & Gaglioti, B. V. (2013). Ice-age megafauna in Arctic Alaska: Extinction, invasion, survival. *Quaternary Science Reviews*, 70, 91–108. <https://doi.org/10.1016/j.quascirev.2013.03.015>
- Mann, D. H., Groves, P., Reanier, R. E., Gaglioti, B. V., Kunz, M. L., & Shapiro, B. (2015). Life and extinction of megafauna in the ice-age Arctic. *Proceedings of the National Academy of Sciences of the United States of America*, 112, 1–6. <https://doi.org/10.1073/pnas.1516573112>
- Mardanov, A. V., Bulygina, E. S., Nedoluzhko, A. V., Kadnikov, V. V., Beletskii, A. V., Tsygankova, S. V., Tikhonov, A. N., Ravin, N. V., Prokhorchuk, E. B., & Skryabin, K. G. (2012). Molecular analysis of the intestinal microbiome composition of mammoth and woolly rhinoceros. *Doklady Biochemistry and Biophysics*, 445, 203–206. <https://doi.org/10.1134/S1607672912040060>
- Meltzer, D. J. (2020). Overkill, glacial history, and the extinction of North America's ice age megafauna. *Proceedings of the National Academy of Sciences of the United States of America*, 1–9, 28555–28563. <https://doi.org/10.1073/pnas.2015032117>
- Meyer, M., & Kircher, M. (2010). Illumina sequencing library preparation for highly multiplexed target capture and sequencing. *Cold Spring Harbor Protocols*, 2010, pdb.prot5448. <https://doi.org/10.1101/pdb.prot5448>
- Miller, J. H., & Simpson, C. (2022). When did mammoths go extinct? *Nature*, 612, E1–E3. <https://doi.org/10.1038/s41586-022-05416-3>
- Mitra, S., Gilbert, J. A., Field, D., & Huson, D. H. (2010). Comparison of multiple metagenomes using phylogenetic networks based on ecological indices. *The ISME Journal*, 4, 1236–1242. <https://doi.org/10.1038/ismej.2010.51>
- Monteath, A. J., Gaglioti, B. V., Edwards, M. E., & Froese, D. (2021). Late Pleistocene shrub expansion preceded megafauna turnover and extinctions in eastern Beringia. *Proceedings of the National Academy of Sciences of the United States of America*, 118, e2107977118. <https://doi.org/10.1073/PNAS.2107977118>
- Monteath, A. J., Kuzmina, S., Mahony, M., Calmels, F., Porter, T., Mathewes, R., Sanborn, P., Zazula, G., Shapiro, B., Murchie, T. J., Poinar, H. N., Sadoway, T., Hall, E., Hewitson, S., & Froese, D. (2023). Relict permafrost preserves megafauna, insects, pollen, soils and pore-ice isotopes of the mammoth steppe and its collapse in Central Yukon. *Quaternary Science Reviews*, 299, 107878. <https://doi.org/10.1016/J.QUASCIREV.2022.107878>
- Murchie, T. J. (2021). *Ancient environmental DNA as a means of understanding ecological restructuring during the Pleistocene-Holocene transition in Yukon, Canada*. McMaster University.
- Murchie, T. J., Karpinski, E., Eaton, K., Duggan, A. T., Baleka, S., Zazula, G., MacPhee, R. D. E., Froese, D., & Poinar, H. N. (2022). Pleistocene mitogenomes reconstructed from the environmental DNA of permafrost sediments. *Current Biology*, 32, 851–860. <https://doi.org/10.1016/J.CUB.2021.12.023>
- Murchie, T. J., Kuch, M., Duggan, A. T., Ledger, M. L., Roche, K., Klunk, J., Karpinski, E., Hackenberger, D., Sadoway, T., MacPhee, R., Froese, D., & Poinar, H. (2021). Optimizing extraction and targeted capture of ancient environmental DNA for reconstructing past environments using the PalaeoChip Arctic-1.0 bait-set. *Quaternary Research*, 99, 305–328. <https://doi.org/10.1017/qua.2020.59>
- Murchie, T. J., Monteath, A. J. A. J., Mahony, M. E., Long, G. S., Cocker, S., Sadoway, T., Karpinski, E., Zazula, G., MacPhee, R. D. E., Froese, D., Poinar, H. N., Cocker, S., Sadoway, T., Zazula, G., MacPhee, R. D. E.,
- Froese, D., & Poinar, H. N. (2021). Collapse of the mammoth-steppe in Central Yukon as revealed by ancient environmental DNA. *Nature Communications*, 1–18, 7120. <https://doi.org/10.1038/s41467-021-27439-6>
- O'Leary, N. A., Wright, M. W., Brister, J. R., Ciuffo, S., Haddad, D., McVeigh, R., Rajput, B., Robbertse, B., Smith-White, B., Akoto-Adjei, D., Astashyn, A., Badretdin, A., Bao, Y., Blinkova, O., Brover, V., Chetvernin, V., Choi, J., Cox, E., Ermolaeva, O., ... Pruitt, K. D. (2016). Reference sequence (RefSeq) database at NCBI: Current status, taxonomic expansion, and functional annotation. *Nucleic Acids Research*, 44, D733–D745. <https://doi.org/10.1093/NAR/GKV1189>
- Ouwerkerk, D., Gilbert, R. A., & Klieve, A. (2011). *Archaeophage therapy to control rumen methanogens*. Meat & Livestock Australia Limited.
- Pavelková Říčánková, V., Robovský, J., & Riegert, J. (2014). Ecological structure of recent and last glacial mammalian faunas in northern Eurasia: The case of Altai-Sayan refugium. *PLoS One*, 9, e85056. <https://doi.org/10.1371/journal.pone.0085056>
- Pedersen, M. W., De Sanctis, B., Saremi, N. F., Shapiro, B., & Durbin, R. (2021). Environmental genomics of late Pleistocene black bears and giant short-faced bears. *Current Biology*, 31, 1–9. <https://doi.org/10.1016/j.cub.2021.04.027>
- Pedersen, M. W., Overballe-petersen, S., Ermini, L., Sarkissian, C., Haile, J., Hellstrom, M., Spens, J., Thomsen, P. F., Bohmann, K., Cappellini, E., Schnell, I. B., Wales, N. A., Carøe, C., Campos, F., Schmidt, A. M. Z., Gilbert, M. T. P., Hansen, A. J., Orlando, L., & Willerslev, E. (2015). Ancient and modern environmental DNA. *Philosophical Transactions of the Royal Society of London. Series B, Biological Sciences*, 370, 1–11. <https://doi.org/10.1098/rstb.2013.0383>
- Pester, M., Brambilla, E., Alazard, D., Rattei, T., Weinmaier, T., Han, J., Lucas, S., Lapidus, A., Cheng, J. F., Goodwin, L., Pitluck, S., Peters, L., Ovchinnikova, G., Teshima, H., Detter, J. C., Han, C. S., Tapia, R., Land, M. L., Hauser, L., ... Loy, A. (2012). Complete genome sequences of *Desulfosporosinus orientis* DSM765T, *Desulfosporosinus youngiae* DSM17734T, *Desulfosporosinus meridiei* DSM13257T, and *Desulfosporosinus acidiphilus* DSM22704T. *Journal of Bacteriology*, 194, 6300–6301. <https://doi.org/10.1128/JB.01392-12>
- Popov, I. (2020). The current state of Pleistocene Park, Russia (an experiment in the restoration of megafauna in a boreal environment). *Holocene*, 30, 1471–1473. <https://doi.org/10.1177/0959683620932975>
- Porter, T. J., Schoenemann, S. W., Davies, L. J., Steig, E. J., Bandara, S., & Froese, D. G. (2019). Recent summer warming in northwestern Canada exceeds the Holocene thermal maximum. *Nature Communications*, 10, 1–10. <https://doi.org/10.1038/s41467-019-09622-y>
- Rasmussen, S. O., Andersen, K. K., Svensson, A. M., Steffensen, J. P., Vinther, B. M., Clausen, H. B., Siggaard-Andersen, M. L., Johnsen, S. J., Larsen, L. B., Dahl-Jensen, D., Bigler, M., Röhlisberger, R., Fischer, H., Goto-Azuma, K., Hansson, M. E., & Ruth, U. (2006). A new Greenland ice core chronology for the last glacial termination. *Journal of Geophysical Research-Atmospheres*, 111, 1–16. <https://doi.org/10.1029/2005JD006079>
- Rea, S., Bowman, J. P., Popovski, S., Pimm, C., & Wright, A. D. G. (2007). *Methanobrevibacter millerae* sp. nov. and *Methanobrevibacter olleyae* sp. nov., methanogens from the ovine and bovine rumen that can utilize formate for growth. *International Journal of Systematic and Evolutionary Microbiology*, 57, 450–456. <https://doi.org/10.1099/IJS.0.63984-0>
- Sadoway, T. R. (2014). *A metagenomic analysis of ancient sedimentary DNA across the Pleistocene-Holocene transition*. McMaster University.
- Saidi-Mehrabad, A., Neuberger, P., Hajhosseini, M., Froese, D., & Lanoil, B. D. (2020). Permafrost microbial community structure changes across the Pleistocene-Holocene boundary. *Frontiers in*

- Environmental Science*, 8, 133. <https://doi.org/10.3389/FENVS.2020.00133>
- Schumann, P., Prauser, H., Rainey, F. A., Stackebrandt, E., & Hirsch, P. (1997). Friedmanniella Antarctica gen. Nov., sp. nov., an LL-diaminopimelic acid-containing actinomycete from Antarctic sandstone. *International Journal of Systematic Bacteriology*, 47, 278–283. <https://doi.org/10.1099/00207713-47-2-278>
- Shin, Y., Lee, B. H., Lee, K. E., & Park, W. (2020). *Pseudarthrobacter psychrotolerans* sp. nov., a cold-adapted bacterium isolated from Antarctic soil. *International Journal of Systematic and Evolutionary Microbiology*, 70, 6106–6114. <https://doi.org/10.1099/IJSEM.0.004505>
- Signor, P. W., & Lipps, J. H. (1982). Sampling bias, gradual extinction patterns and catastrophes in the fossil record. *GSA Special Papers*, 190, 291–296.
- Smith, C. I., Chamberlain, A. T., Riley, M. S., Stringer, C., & Collins, M. J. (2003). The thermal history of human fossils and the likelihood of successful DNA amplification. *Journal of Human Evolution*, 45, 203–217. [https://doi.org/10.1016/S0047-2484\(03\)00106-4](https://doi.org/10.1016/S0047-2484(03)00106-4)
- Smith, F. A., Hammond, J. I., Balk, M. A., Elliott, S. M., Lyons, S. K., Pardi, M. I., Tomé, C. P., Wagner, P. J., & Westover, M. L. (2015). Exploring the influence of ancient and historic megaherbivore extirpations on the global methane budget. *Proceedings of the National Academy of Sciences of the United States of America*, 113, 874–879. <https://doi.org/10.1073/pnas.1502547112>
- Spasov, E., Tsuji, J. M., Hug, L. A., Doxey, A. C., Sauder, L. A., Parker, W. J., & Neufeld, J. D. (2020). High functional diversity among Nitrospira populations that dominate rotating biological contactor microbial communities in a municipal wastewater treatment plant. *The ISME Journal*, 14, 1857–1872. <https://doi.org/10.1038/s41396-020-0650-2>
- Stuart, A. J. (2015). Late quaternary megafaunal extinctions on the continents: A short review. *Geological Journal*, 50, 414–433. <https://doi.org/10.1002/gj>
- Thomas, C. M., Desmond-Le Quéméner, E., Gribaldo, S., & Borrel, G. (2022). Factors shaping the abundance and diversity of the gut archaeome across the animal kingdom. *Nature Communications*, 13(1). <https://doi.org/10.1038/s41467-022-31038-4>
- van Bergeijk, D. A., Augustijn, H. E., Elsayed, S. S., Willemse, J., Carrión, V. J., Urem, M., Grigoreva, L. V., Cheprasov, M. Y., Wintermans, B., Budding, A. E., Spaink, H. P., Medema, M. H., & van Wezel, G. P. (2022). Taxonomic and metabolic diversity of actinobacteria isolated from faeces of a 28,000-year-old mammoth. *bioRxiv*. <https://doi.org/10.1101/2022.12.22.521380>
- Vartanyan, S. L., Arslanov, K. A., Karhu, J. A., Possnert, G., & Sulerzhitsky, L. D. (2008). Collection of radiocarbon dates on the mammoths (*Mammuthus primigenius*) and other genera of Wrangel Island, Northeast Siberia, Russia. *Quaternary Research*, 70, 51–59. <https://doi.org/10.1016/j.yqres.2008.03.005>
- Vernot, B., Zavala, E. I., Gómez-Olivencia, A., Jacobs, Z., Slon, V., Mafessoni, F., Romagné, F., Pearson, A., Petr, M., Sala, N., Pablos, A., Aranbur, A., De Castro, J. M. B., Carbonell, E., Li, B., Krajcarz, M. T., Krivoshapkin, A. I., Kolobova, K. A., Kozlikin, M. B., ... Meyer, M. (2021). Unearthing Neanderthal population history using nuclear and mitochondrial DNA from cave sediments. *Science*, 372, eabf1667. <https://doi.org/10.1126/SCIENCE.ABF1667>
- Vishnivetskaya, T. A. (2009). Viable cyanobacteria and green algae from the permafrost darkness. In R. Margesin (Ed.), *Permafrost soils* (pp. 73–84). Springer.
- Vishnivetskaya, T. A., Almatari, A. L., Spirina, E. V., Wu, X., Williams, D. E., Pfiffner, S. M., & Rivkina, E. M. (2020). Insights into community of photosynthetic microorganisms from permafrost. *FEMS Microbiology Ecology*, 96, 229. <https://doi.org/10.1093/FEMSEC/FIAA229>
- Wang, R., Wang, M., Wang, J., & Lin, Y. (2021). Habitats are more important than seasons in shaping soil bacterial communities on the Qinghai-Tibetan plateau. *Microorganisms*, 9, 1595. <https://doi.org/10.3390/MICROORGANISMS9081595>
- Wang, Y., Pedersen, M. W., Alsos, I. G., De Sanctis, B., Racimo, F., Prohaska, A., Coissac, E., Owens, H. L., Merkel, M. K. F., Fernandez-Guerra, A., Rouillard, A., Lammers, Y., Alberti, A., Denoeud, F., Money, D., Ruter, A. H., McColl, H., Larsen, N. K., Cherezova, A. A., ... Willerslev, E. (2021). Late quaternary dynamics of Arctic biota from ancient environmental genomics. *Nature*, 600, 86–92. <https://doi.org/10.1038/s41586-021-04016-x>
- Wang, Y., Prohaska, A., Dong, H., Alberti, A., Alsos, I. G., Beilman, D. W., Bjørk, A. A., Cao, J., Cherezova, A. A., Coissac, E., De Sanctis, B., Denoeud, F., Dockter, C., Durbin, R., Edwards, M. E., Edwards, N. R., Esdale, J., Fedorov, G. B., Fernandez-Guerra, A., ... Willerslev, E. (2022). Reply to: When did mammoths go extinct? *Nature*, 612, E4–E6. <https://doi.org/10.1038/s41586-022-05417-2>
- Weese, J. S., Shury, T., & Jelinski, M. D. (2014). The fecal microbiota of semi-free-ranging wood bison (*Bison bison athabascae*). *BMC Veterinary Research*, 10, 1–8. <https://doi.org/10.1186/1746-6148-10-120>
- Weimer, P. J., & Zeikus, J. G. (1978). Acetate metabolism in *Methanosarcina barkeri*. *Archives of Microbiology*, 119, 175–182. <https://doi.org/10.1007/BF00964270>
- Willerslev, E., Davison, J., Moora, M., Zobel, M., Coissac, E., Edwards, M. E., Lorenzen, E. D., Vestergard, M., Gussarova, G., Haile, J., Craine, J., Gielly, L., Boessenkool, S., Epp, L. S., Pearman, P. B., Cheddadi, R., Murray, D., Brathen, K. A., Yoccoz, N., ... Taberlet, P. (2014). Fifty thousand years of Arctic vegetation and megafaunal diet. *Nature*, 506, 47–51. <https://doi.org/10.1038/nature12921>
- Woo, M. K. (2012). *Permafrost hydrology*. Springer.
- Zaitseva, S., Badmaev, N., Kozyreva, L., Dambaev, V., & Barkhutova, D. (2022). Microbial community in the permafrost thaw gradient in the south of the Vitim plateau (Buryatia, Russia). *Microorganisms*, 10, 2202. <https://doi.org/10.3390/MICROORGANISMS10112202/S1>
- Zavala, E. I., Jacobs, Z., Vernot, B., Shunkov, M. V., Kozlikin, M. B., Derevianko, A. P., Essel, E., de Filippo, C., Nagel, S., Richter, J., Romagné, F., Schmidt, A., Li, B., O'Gorman, K., Slon, V., Kelso, J., Pääbo, S., Roberts, R. G., & Meyer, M. (2021). Pleistocene sediment DNA reveals hominin and faunal turnovers at Denisova cave. *Nature*, 1–5, 399–403. <https://doi.org/10.1038/s41586-021-03675-0>
- Zazula, G. D., Froese, D. G., Schweger, C. E., Mathewes, R. W., Beaudoin, A. B., Telka, A. M., Harrington, C. R., & Westgate, J. A. (2003). Ice-age steppe vegetation in east Beringia. *Nature*, 423, 603. <https://doi.org/10.1038/423603a>
- Zazula, G. D., Hall, E., Hare, P. G., Thomas, C., Mathewes, R., Farge, C., Martel, A. L., Heintzman, P. D., & Shapiro, B. (2017). A middle Holocene steppe bison and paleoenvironments from the ver-sleuce meadows, Whitehorse, Yukon, Canada. *Canadian Journal of Earth Sciences*, 54, 1138–1152. <https://doi.org/10.1139/cjes-2017-0100>
- Zhang, D., Xia, H., Chen, F., Li, B., Slon, V., Cheng, T., Yang, R., Jacobs, Z., Dai, Q., Massilani, D., Shen, X., Wang, J., Feng, X., Cao, P., Yang, M. A., Yao, J., Yang, J., Madsen, D. B., Han, Y., ... Fu, Q. (2020). Denisovan DNA in late Pleistocene sediments from Baishiya karst cave on the Tibetan plateau. *Science*, 370, 584–587. <https://doi.org/10.1126/science.abb6320>
- Zhou, J., Holmes, D. E., Tang, H. Y., & Lovley, D. R. (2021). Correlation of key physiological properties of *Methanosarcina* isolates with environment of origin. *Applied and Environmental Microbiology*, 87, 1–15. <https://doi.org/10.1128/AEM.00731-21>
- Zhou, M., O'Hara, E., Tang, S., Chen, Y., Walpole, M. E., Górká, P., Penner, G. B., & Guan, L. L. (2021). Accessing dietary effects on the rumen microbiome: Different sequencing methods tell different stories. *Veterinary Sciences*, 8, 138. <https://doi.org/10.3390/VETSCI8070138/S1>

- Zimov, S. A. (2005). Pleistocene park: Return of the mammoth's ecosystem. *Science*, 308, 796–798. <https://doi.org/10.1126/science.1113442>
- Zimov, S. A., Zimov, N. S., Tikhonov, A. N., & Chapin, I. S. (2012). Mammoth steppe: A high-productivity phenomenon. *Quaternary Science Reviews*, 57, 26–45. <https://doi.org/10.1016/j.quascirev.2012.10.005>

SUPPORTING INFORMATION

Additional supporting information can be found online in the Supporting Information section at the end of this article.

How to cite this article: Murchie, T. J., Long, G. S., Lanoil, B. D., Froese, D., & Poinar, H. N. (2023). Permafrost microbial communities follow shifts in vegetation, soils, and megafauna extinctions in Late Pleistocene NW North America. *Environmental DNA*, 5, 1759–1779. <https://doi.org/10.1002/edn3.493>